

**Nonlocal Field Theories at Finite Temperature and
Density**

**A THESIS
SUBMITTED TO THE FACULTY OF THE GRADUATE SCHOOL
OF THE UNIVERSITY OF MINNESOTA
BY**

Abraham Subba Reddy

**IN PARTIAL FULFILLMENT OF THE REQUIREMENTS
FOR THE DEGREE OF
Doctor of Philosophy**

Joseph I. Kapusta, Advisor

May, 2014

© Abraham Subba Reddy 2014
ALL RIGHTS RESERVED

Acknowledgements

I would first like to thank my advisor Joseph Kapusta for all of his valuable advice and especially for his patience with me through this journey. I would also like to thank Tirthabir Biswas for all of the time he spent working with me and for being willing to help whenever he could. Finally, I would like to thank my fellow graduate students for making this chapter of my life an enjoyable one.

Dedication

To my mother Terry and grandmother Phyllis.

Abstract

In this thesis we investigate nonlocal fields in physics at finite temperature and density. We first investigate the thermodynamic properties of a nonlocal tachyon motivated by the nonlocal structure in string field theory. We use previously developed perturbative methods for nonlocal fields to calculate the partition function and the equation of state in the high temperature limit. We find that in these models the tachyons undergo a second order phase transition. We compare our results with those of ordinary scalar field theory. We also calculate the one loop finite temperature effective potential. We then investigate a nonlocally modified effective field theory for nuclear matter. We pay particular attention to the effect of the modification on the two-loop diagrams. We then compare to the conventional case. We find that while we do end up with a softer behavior in the loop contributions this leads to only a minor reduction in the magnitude of the coupling constants.

Contents

Acknowledgements	i
Dedication	ii
Abstract	iii
List of Tables	vi
List of Figures	vii
1 Introduction	1
2 Nonlocal Scalar at Finite Temperature	3
2.1 Introduction	3
2.2 Action and Critical Temperature	7
2.2.1 Action	7
2.2.2 Critical Temperature	10
2.3 Equation of State	13
2.3.1 Formalism	13
2.3.2 Sums and Integrals	18
2.3.3 Equation of State for $M, T \gg \mu$	21
2.4 Numerical Results and Comparison to Local Field Theory	23
2.5 Effective Potential	27
2.6 Conclusion	34

3	Review of Nuclear Matter	36
3.1	Introduction	36
3.2	Walecka Model	37
3.2.1	Relativistic Hartree	39
3.2.2	QHD II MFT	40
3.3	Two-loop Diagrams	42
4	Nonlocal effective model	47
4.1	Introduction	47
4.2	Nonlocal Model	48
4.2.1	MFT and Hartree Approximation	48
4.2.2	Two-loop diagrams	49
4.2.3	QHD-II	53
4.3	Numerical Work	55
4.4	Conclusion	61
5	Conclusion and Discussion	63
	References	64
	Appendix A. Theta Functions	71
	Appendix B. Nonlocal Fermion	73
B.1	Nonlocal Fermion	73
B.1.1	Conserved Current	74
B.1.2	The partition function	76
	Appendix C. Propagator Pole Structure	79
C.1	Finite Temperature	79
C.2	Zero Temperature Limit	80

List of Tables

4.1	Parameter Sets	57
-----	--------------------------	----

List of Figures

2.1	The vacuum potential V in dimensionless form.	9
2.2	Two-loop contribution to $\ln Z$ including combinatoric factors and the counter-term.	15
2.3	One loop contribution to the self-energy including combinatoric factors and the counter-term.	15
2.4	Scaling of the critical temperature with the parameters. The dependence changes from square-root to linear around $T_c/M \sim 0.4$	26
2.5	Dependence of the effective mass on temperature for $T_c/M = 1/100$ (dashed/red) and $T_c/M = 10$ (solid/blue).	27
2.6	The interaction measure as a function of temperature for $T_c/M = 1/100$ (dashed/red) and $T_c/M = 10$ (solid/blue).	28
2.7	Discontinuity in the heat capacity at the critical temperature.	28
2.8	Effective potential for $T_c/M = 1/100$ at $T/T_c=0.5$ (solid/blue), 1.0 (dash-dotted/black), and 1.5 (dashed/red).	33
2.9	Effective potential for $T_c/M = 10$ at $T/T_c=0.5$ (solid/blue), 1.0 (dash-dotted/black), and 1.5 (dashed/red).	34
3.1	Two loop diagrams for scalar and vector	42
3.2	2-loop Contributions	44
3.3	Two loop contributions with point vertices. $g_\sigma^2 = 54.3$, $m_\sigma=458$ MeV, $g_\omega^2=102.8$, $m_\omega=783$ MeV [46]	45
3.4	Two loop contributions with form factor. [46]	46
4.1	Scalar(dotted) and Vector(wavy) interaction vertices	49
4.2	ρ interaction vertex	53
4.3	Two loop diagrams for the rho	54

4.4	Comparison of the usual two-loop σ and ω contribution (blue) with the nonlocal one (red). At the equilibrium value of 1.3 fm^{-1} we find a reduction of about 8%	57
4.5	Comparison of the one-loop energy (green) with the total two-loop energy with the σ and ω (blue,dotdashed)	58
4.6	Adjustment of couplings to fit total energy to nuclear equilibrium. One-loop (green). Total two-loop energy with the σ and ω (blue, dotdashed)	58
4.7	Two-loop exchange contribution comparison for the π . Conventional (blue-dotted). Nonlocal (red-dashed).	59
4.8	Total energy including the the σ, ω, π . Two-loop contributions (red-dotdashed) compared with RHA (green-dashed)	59
4.9	Effective Mass determined at the one loop level (red,solid) and two-loop level (blue,dotdashed)	60
4.10	Two-loop exchange contribution for the nonlocal ρ meson	60
4.11	Comparison of one-loop energy (green-dashed) with the total two-loop including the $\sigma, \omega, \pi, \rho$ (purple-large dashed)	61

Chapter 1

Introduction

Nonlocal quantum field theories have been considered for almost as long as quantum field theory itself. As far back as the 1950's Hideki Yukawa was considering these theories as an alternative to the usual point particle description. In a two paper series, he investigated the possibility of removing divergences by taking into account the finite size of elementary particles[1].

Since then, nonlocal fields have been investigated in a variety of contexts. An excellent example of this is work done by John Moffat and collaborators [22] starting in the 90's. He investigated the possibility of a nonlocal alternative to the Standard Model. In much of his work he investigated an ultraviolet complete quantum field theory with nonlocal interactions. Another interesting exploration by Evans, Moffat, Kleppe and Woodard was the use of nonlocal regularizations of gauge theories [3].

One of Moffat's coloborators, Woodard, along with Deser went on to explore a nonlocally modified gravity model inspired by quantum loop corrections [2]. In this instance, they were able to avoid some of the fine tuning necessary in the standard cosmological models. They also postulated that theories of this kind may be useful to the black hole information problem

Much of the more recent work has come in the context of String Field Theory. As we will discuss in more detail in Chapter 2, there are a plethora of nonlocal theories derived in different ways from SFT. Many of these theories have been investigated for their cosmological implications.

As evidenced by the above there is a rich history of exploring the applications of

nonlocal fields in a variety of contexts. In this thesis we will follow in this tradition.

This thesis is organized as follows:

- In Chapter 2 we consider the action for a nonlocal scalar whose form is motivated by String Field Theory. We begin by giving the finite temperature formulation of the model. We then show that a second order phase transition occurs at high temperatures and we estimate the critical temperature. We continue by employing perturbation theory to calculate the one and two-loop contributions to the partition function which allows us to find the equation of state about the true minimum of the potential. Comparisons are made to the local scalar case and numerical results are then presented. Finally we calculate the one-loop effective potential for the model. The work contained in this chapter was published in [4].
- In Chapter 3 we review the conventional model for relativistic nuclear matter which contains nucleons interacting via the σ and ω mesons. This is known as the Walecka Model or Quantum Hydrodynamics I. We first discuss the model at the mean field level. The π and ρ mesons are then included which is known as QHD II. We then review the calculations of the two-loop contributions found in the literature. We discuss the issues with the size of the loop contributions and solutions to this that have been previously proposed.
- In Chapter 4 we begin by motivating our nonlocally modified model for nuclear matter that addresses some of the issues discussed in Chapter 3. In the mean field our theory yields the same results as the conventional theory. We then proceed to investigate the two-loop contributions for the σ , ω , π and ρ mesons. We compare the results of the two-loop energy to that of the one-loop result. We then show that the coupling constants can be refit to reproduce nuclear matter properties. Numerical results are presented and discussed.

Chapter 2

Nonlocal Scalar at Finite Temperature

2.1 Introduction

Tachyons are ubiquitous in string theory. They made their first appearance in closed bosonic string theory. Since then, they have been found to exist as open string excitations in the world volume of D-branes in bosonic theories and in non-BPS D-branes in superstring theory, as well as excitations in brane–anti-brane systems; see [5] for a review. In conventional field theory the appearance of a tachyon usually implies that we are perturbing around an unstable vacuum; the system should evolve to its true vacuum with positive mass-squared around which we can perform perturbative quantum calculations meaningfully. There is growing evidence to suggest the same is true in string theory [5, 6]. For instance, the open string tachyons are thought to represent the instability in the various D-brane systems. The rolling of the tachyon from the unstable potential hill to its stable minimum then describes the dissolution of the unstable D-branes into closed string excitations around the true vacuum which no longer supports open string excitations. This process is often referred to as tachyon condensation in the string literature. While the classical dynamics of the above process has been studied extensively, relatively little attention have been paid to the quantum theory of the tachyon.

In the current section, we will study thermodynamic properties of a class of nonlocal

actions which, at least superficially, resembles the nonlocal action for the string field theory tachyons. To be more precise, the action we will consider is what one obtains in the simplest level of truncation in the String Field Theory (SFT) approach [7] where only the tachyon field is kept [8]. Our main interest will be to study whether the tachyon is stable above some critical temperature, which would imply that the brane configuration is stable. If this is the case, then we have the possibility to study how the branes become unstable when the temperature drops below that critical value, leading to eventual dissolution of the branes. Our analysis will demonstrate that, just as in ordinary field theory, one can consistently perform quantum calculations of the partition function in such nonlocal models to address these type of questions.

We would like to emphasize that while work done on such simplified level-truncated string-inspired nonlocal models have been fruitful in elucidating certain aspects of string theory [9]-[14], when considering temperatures above the string scale one expects all the string states to contribute to the partition function which our analysis does not account for¹. In particular, this means that we will be unable to capture any physics related to the conjectured stringy Hagedorn phase which is due the exponential growth of the spectrum of physical string states. Also, in the real string theory the mass of the tachyon is of the same order of magnitude as the string scale. For phenomenological reasons we will keep the mass of the tachyon arbitrary throughout the paper and, due to technicalities, we have only performed our calculations when the tachyon is much lighter than the string scale. For all these reasons the analysis and results presented in this paper may be of limited direct relevance to understanding the thermal properties of the complete SFT. However, we believe that the formalism and the computational techniques we have developed will help us to consider realistic stringy models in the future. With regard to understanding quantum phenomenon in string theory it is worth noting that similar nonlocal models, such as p-adic strings [31], have been shown to reproduce properties such as thermal-duality [32] (which has been variously argued in the string literature [33]) and Regge behavior [34]-[35].

To understand the origin of the nonlocal structure we will consider in our models, let us look at the SFT action. Schematically, the string field Ψ can be thought of as a matrix-valued 1-form [8] with a Chern-Simons type action. The bosonic SFT action,

¹ Our results for temperatures below the string scale should still provide insights into thermal SFT.

for instance, is then given by

$$S = \frac{1}{2\alpha'} \int \Psi \star Q\Psi + \frac{g}{3} \int \Psi \star \Psi \star \Psi \quad (2.1.1)$$

where Q is the BRST operator which is normalized to provide canonical kinetic terms to the various particle fields contained in the SFT spectrum, g is the string coupling constant, and $1/\sqrt{\alpha'}$ is the string tension. The \star product has the effect of diffusing or smearing out the interaction over the string length. For instance, if f corresponds to a canonically normalized particle field in the SFT spectrum, then an interaction term involving the \star product in the string field Ψ translates into interactions for f where they only enter in momentum-dependent combinations

$$\tilde{f} = \exp \left[\alpha' \ln(3\sqrt{3}/4) \square \right] f$$

Equivalently, one can work with the redefined fields \tilde{f} in terms of which the interactions have the usual polynomial form, but the kinetic operator picks up the nonlocal exponential derivative dependence [8]. Thus, if we keep only the tachyon field, then the corresponding field theory action has the form

$$S = \int d^4x \left[\frac{1}{2} \phi e^{-\square/M^2} (\square - m^2) \phi - V(\phi) \right] \quad (2.1.2)$$

where m^2 is the mass of the tachyon at the maximum, and M is the scale of nonlocality that describes stringy interactions. Both m and M are proportional to the string tension. For example, for the bosonic SFT $m^2 = -1/\alpha'$, while $M^2 \sim 1/\alpha' \ln(3\sqrt{3}/4)$. We will treat m and M as independent parameters for technical and phenomenological reasons. The $V(\phi)$ represents a polynomial interaction, typically cubic or quartic.

We employ finite temperature methods that were developed for such nonlocal theories in [36, 32] to investigate the thermodynamic properties of the tachyonic excitations. We will discover that, just as in ordinary Quantum Field Theory (QFT), the nonlocal tachyon undergoes a second order phase transition. The effect of the stringy nonlocality seems to weaken the phase transition. This means that the discontinuity in the specific heat as one approaches the critical temperature from above and below decreases as M decreases. We emphasize that the QFT limit is expected to be attained in the limit $M \rightarrow \infty$, and we explicitly verify that this is indeed the case. In this paper we work in the limit $M \gg m$; that is, we are close to the particle limit, but the formalism and

techniques that we have developed can be employed to understand the (perhaps) more interesting and relevant situation where $M \sim m$.

Another important motivation for considering such theories is to explore phenomenological applications to particle physics. For instance, our calculations help to clarify the relation between the conventional QFT, which is based on a renormalization prescription, and the string inspired nonlocal actions where loop diagrams are typically finite. Intuitively, the exponential cut-off scale, M^2 , acts as a Lorentz-invariant physical regulator. The expressions for the various thermodynamic quantities in these nonlocal models are almost identical to what one obtains using traditional renormalization prescription, except that there are corrections which are suppressed as $\mathcal{O}[\exp(-M^2/4T^2)]$. This happens because one takes the limit $M \rightarrow \infty$ *after* imposing the “renormalization conditions”, according to the standard renormalization prescription, whereas the M in stringy Lagrangians is a finite physical parameter encoding the nonlocality of the model. This opens up possibilities for phenomenological applications in particle physics if M is close enough to the scale of Standard Model physics. For one proposed alternative to the Standard Model using SFT-type actions see [22].

Another goal is also to pave the way for possible connections between string theory and cosmology. For previous applications of nonlocal models to cosmology see [15]-[21]. (For related work on nonlocal gravity see [22]-[30].) In recent years, string thermodynamics has found several applications in the early Universe cosmology [37]. In particular, there have been efforts to see whether stringy thermal fluctuations can play a role in the formation of the anisotropies in the Cosmic Microwave Background Radiation (CMBR). There are also the so-called warm inflationary scenarios where particles are continuously produced and which then thermalize and influence inflationary dynamics, both at the level of the background and the fluctuations [38]. It would be interesting to consider similar scenarios where stringy excitations are produced instead, potentially providing a prospect to observe stringy properties in CMBR. Our calculations would be relevant for such a discussion.

The chapter is organized as follows: In section 2, we introduce the nonlocal model and its finite temperature formulation. By calculating the temperature dependence of the effective mass and minimum of the potential, we demonstrate that a second order phase transition occurs in the nonlocal models under consideration at high temperature,

and estimate the critical temperature. In section 3, we follow the traditional perturbation theory approach to calculate the one and two-loop diagrams contributing to the partition function of the tachyon. This enables us to obtain the equation of state for the thermal excitations of the tachyons around the true minimum. The same techniques can be used to calculate N-point diagrams for arbitrary values of N at high temperature. This is sufficient for us to obtain the critical temperature and determine the nature of the phase transition. In section 4, we summarize the analytical computations and provide numerical results. This enables us to compare the equation of state in the nonlocal models with the analogous local QFT equation of state. In section 5, we calculate the 1-loop effective potential which extrapolates away from the equilibrium states. Concluding remarks are contained in section 6.

2.2 Action and Critical Temperature

In this section we introduce the nonlocal action and show that a second order phase transition is to be expected at high temperature. More elaborate calculations of the equation of state and of the effective potential follow in sections 3, 4 and 5.

2.2.1 Action

Our starting point is the SFT type action given by [18]

$$S = \int d^4x \left[\frac{1}{2} \phi e^{-\square/M^2} (\square - m^2) \phi - V(\phi) \right] \quad (2.2.1)$$

The metric is such that $\square = -\partial_t^2 + \nabla^2$. In the bosonic cubic string field theory the action for the tachyon is of the above form with $V(\phi) \propto \phi^3$, while for the supersymmetric case one expects a quartic potential. In either case the mass-squared term is always negative, $m^2 < 0$, indicating the presence of a tachyon at $\phi = 0$. In this paper we focus on the quartic coupling

$$V(\phi) = \lambda \phi^4 \quad (2.2.2)$$

In SFT λ is proportional to g^2 . Since the potential is bounded from below, we expect to be able to perform loop calculations without encountering any pathologies. In this context we note that although the presence of higher derivative terms usually indicate

the existence of additional ghost-like states, the fact that in the SFT action they combine into an exponential ensures that there are no extra poles in the propagator. Thus there are, in fact, no additional physical states, ghosts or otherwise. There are also strong arguments to suggest that the initial value problem in these models are well defined, and classical trajectories can be uniquely specified by only a finite set of parameters [39].

There are two interesting limits of the action expressed by eq. (2.2.1). When m is fixed and $M \rightarrow \infty$, one recovers the conventional local field theory action for a scalar field. When M is fixed and $m \rightarrow \infty$, one recovers the p -adic field theory [31]. In this paper we consider the case when both m and M are finite but with $|m| \ll M$.

Application of the usual finite temperature formalism to nonlocal actions involving an infinite series of higher derivative terms, such as (2.2.1), have been studied recently [32]. The basic prescription is rather straightforward and resembles the finite temperature methods implemented in usual local quantum field theories. The main difference is that the propagator gets modified by the presence of the nonlocal terms, and ultraviolet divergences in the quantum loops are either softened or eliminated altogether. In some sense the mass parameter M acts as an ultraviolet cutoff. Thus the renormalization prescription is somewhat modified from the usual field theories.

One of the important differences between SFT-type theories and p -adic theory is that, in the latter case, $\phi = 0$ corresponds to a minimum while in the SFT-type case it is a maximum, hence perturbative calculations around $\phi = 0$ are not well-defined. (This is elaborated on in more detail in the following sections.) To perform quantum loop calculations we must expand around the true minimum. At the classical, or tree, level the minimum is located at $\phi_0 = \mu/2\sqrt{\lambda}$, where we have defined $\mu^2 \equiv -m^2 > 0$. See Fig. 1. However, at finite temperature the minimum is shifted to smaller values of ϕ . To account for this we expand around the true minimum, $v(T)$:

$$\phi = v(T) + \phi_f \tag{2.2.3}$$

where $v(T)$ is independent of space and time but does depend on the temperature, while ϕ_f is the fluctuation around it whose average value is zero. When doing loop calculations using the fluctuation ϕ_f around the average value of the field $v(T)$ at the temperature T , we should use the dressed propagator (or our best estimate of it) and not

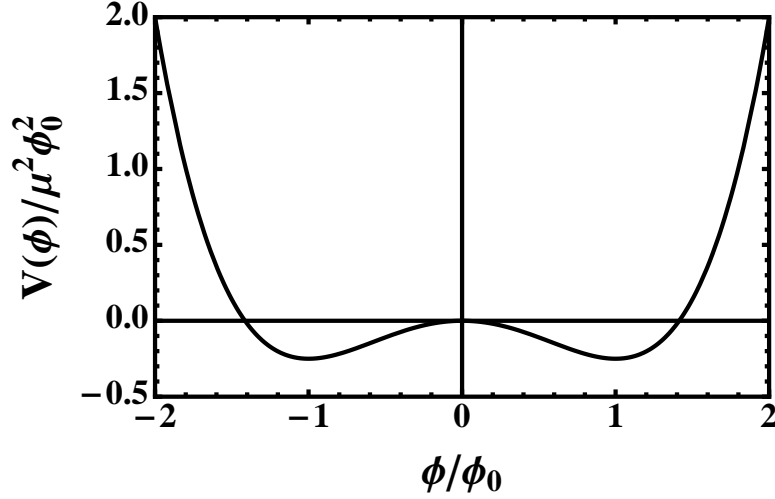


Figure 2.1: The vacuum potential V in dimensionless form.

the bare propagator. As in conventional models of spontaneously broken symmetries in local field theory, we will see that as the temperature increases the values of the condensate $v(T)$ and the effective mass both decrease to zero at a critical temperature T_c . This can be done in the usual way by introducing an additional mass-shift δm^2 in the the quadratic part of the action and then subtracting it as a counter-term. Then the Lagrangian reads

$$\mathcal{L} = \mathcal{L}_{\text{quad}} + \mathcal{L}_{\text{int}} + \mathcal{L}_{\text{ct}} - V_{\text{cl}}(v) \quad (2.2.4)$$

where

$$\mathcal{L}_{\text{quad}} = \frac{1}{2}\phi_f \left[e^{-\square/M^2} (\square + \mu^2) - 12\lambda v^2 - \delta m^2 \right] \phi_f \quad (2.2.5)$$

$$\mathcal{L}_{\text{int}} = -4\lambda v \phi_f^3 - \lambda \phi_f^4$$

$$\mathcal{L}_{\text{ct}} = \frac{1}{2}\delta m^2 \phi_f^2$$

$$V_{\text{cl}}(v) = -\frac{1}{2}\mu^2 v^2 + \lambda v^4 \quad (2.2.6)$$

The $v(T)$ and $\delta m^2(T)$ are as yet undetermined functions of the temperature.

2.2.2 Critical Temperature

The functions $v(T)$ and $\delta m^2(T)$ introduced above can be determined by the 1-point and 2-point loop diagrams, respectively. In this section we derive formulas for them at the 1-loop mean-field level. We begin by noting that the thermodynamic potential is given by

$$\Omega = V_{\text{cl}}(v) - \frac{T}{V} \ln \left\{ \int [d\phi_f] \exp \left(\int_0^\beta d\tau \int_V d^3x [\mathcal{L}_{\text{quad}} + \mathcal{L}_{\text{int}} + \mathcal{L}_{\text{ct}}] \right) \right\} \quad (2.2.7)$$

where $\beta = 1/T$ and V is the volume. The thermodynamic potential must be a minimum with respect to variations in v , thus providing an equation to determine $v(T)$. Similarly the function δm^2 is determined by the Schwinger-Dyson equation in the 1-loop mean-field approximation.

According to the formalism that was developed in [32] to compute Feynman diagrams in nonlocal field theories such as (2.2.1), the only diagrammatic rule that needs to change is the propagator. From (2.2.5) we see that

$$\mathcal{D} = \frac{1}{e^{(\omega_n^2 + p^2)/M^2} (\omega_n^2 + p^2 - \mu^2) + 12\lambda v^2 + \delta m^2} \quad (2.2.8)$$

where we have introduced the Matsubara frequencies, $\omega_n = 2n\pi T$, as appropriate for finite temperature field theory [40]. We emphasize the exponential suppression of the propagator at large momenta which is a typical characteristic of these theories and which helps to regulate the ultraviolet divergences of loop diagrams.

Let us now try to compute these quantities at the 1-loop level; a more rigorous comprehensive analysis will be provided in the next two sections.

$$\frac{\partial \Omega}{\partial v} = 0 \quad \Rightarrow \quad (4\lambda v^2 - \mu^2)v + 12\lambda v T \sum_n \int \frac{d^3p}{(2\pi)^3} \mathcal{D} = 0 \quad (2.2.9)$$

where the first term comes from the classical potential while the second term comes from the 1-loop tadpole diagram. For sufficiently small T there is a local maximum at $v = 0$ and a minimum at

$$v^2 = \frac{\mu^2}{4\lambda} - 3T \sum_n \int \frac{d^3p}{(2\pi)^3} \mathcal{D}(\omega_n, p; v, \delta m^2) \quad (2.2.10)$$

At a critical temperature T_c these become degenerate. The value of T_c is determined by

$$T_c = \frac{\mu^2}{12\lambda} \left[\sum_n \int \frac{d^3p}{(2\pi)^3} \mathcal{D} \right]^{-1} \quad (2.2.11)$$

so that above this temperature there is only one minimum at $v = 0$. This temperature will later be identified with the critical temperature of a second order phase transition.

The two equations above are not sufficient to determine $v(T)$ and T_c because the right side depends on \mathcal{D} which itself depends on δm^2 . In the mean-field approximation it is determined by the 1-loop self-energy diagram which involves only the 4-point vertex, not the other diagram involving the 3-point vertices. (For details see the next section.) This is a gap equation.

$$\delta m^2 = 12\lambda T \sum_n \int \frac{d^3p}{(2\pi)^3} \mathcal{D}(\omega_n, p; v, \delta m^2) \quad (2.2.12)$$

Equations (2.2.10) and (2.2.12) are to be solved simultaneously and self-consistently to determine $v(T)$ and $\delta m^2(T)$.

First consider $T > T_c$: the minimum is located at $v = 0$ and so δm^2 can be determined as the solution to the single equation

$$\delta m^2 = 12\lambda T \sum_n \int \frac{d^3p}{(2\pi)^3} \frac{1}{e^{(\omega_n^2 + p^2)/M^2} (\omega_n^2 + p^2 - \mu^2) + \delta m^2} \quad (2.2.13)$$

For $T < T_c$, on the other hand, there is a simple relation between δm^2 and v , namely

$$\delta m^2 = \mu^2 - 4\lambda v^2 \quad (2.2.14)$$

The temperature T_c where v goes to zero is exactly the same temperature where the effective mass

$$m_{\text{eff}}^2 \equiv \delta m^2 - \mu^2 + 12\lambda v^2 = 8\lambda v^2 \quad (2.2.15)$$

goes to zero. The condensate can be determined via

$$v^2 = \frac{\mu^2}{4\lambda} - 3T \sum_n \int \frac{d^3p}{(2\pi)^3} \frac{1}{e^{(\omega_n^2 + p^2)/M^2} (\omega_n^2 + p^2 - \mu^2) + \mu^2 + 8\lambda v^2} \quad (2.2.16)$$

and this in turn allows for the direct algebraic determination of δm^2 .

To obtain simple analytic results, for the moment we shall assume that $\mu \ll M$ and that $M \ll T_c$. These assumptions can of course be relaxed albeit at the expense of numerical calculations, and they will be presented in the following sections. Therefore we focus on temperatures $T \gg M$. In this situation a nonzero Matsubara frequency will contribute an amount which is suppressed by a factor $\exp(-4\pi^2 T^2/M^2)$ and is totally ignorable. Thus

$$T \sum_n \int \frac{d^3 p}{(2\pi)^3} \mathcal{D} \rightarrow \frac{MT}{4\pi\sqrt{\pi}}. \quad (2.2.17)$$

Hence both the condensate v and the effective mass $m_{\text{eff}}^2 = 12\lambda v^2 - \mu^2 + \delta m^2$ must vanish at the same critical temperature given by

$$T_c = \frac{\pi\sqrt{\pi}}{3} \frac{\mu^2}{\lambda M}. \quad (2.2.18)$$

This is strongly indicative of a second order phase transition. For consistency we need $T_c \gg M$. This results in the limit

$$\lambda M^2 \ll \mu^2 \ll M^2. \quad (2.2.19)$$

To summarize: in this limit

$$\begin{aligned} v^2 &= \frac{\mu^2}{4\lambda} - \frac{3MT}{4\pi\sqrt{\pi}} \\ \delta m^2 &= \frac{3\lambda MT}{\pi\sqrt{\pi}} \\ m_{\text{eff}}^2 &= 2\mu^2 - \frac{6\lambda MT}{\pi\sqrt{\pi}} = 8\lambda v^2 \end{aligned} \quad (2.2.20)$$

below T_c and

$$\begin{aligned} v^2 &= 0 \\ \delta m^2 &= \frac{3\lambda MT}{\pi\sqrt{\pi}} \\ m_{\text{eff}}^2 &= \frac{3\lambda MT}{\pi\sqrt{\pi}} - \mu^2 \end{aligned} \quad (2.2.21)$$

above T_c .

2.3 Equation of State

In this section we perform a more sophisticated analysis of the equation of state. We proceed analytically as far as possible and defer numerical calculations to a later section. Readers primarily interested in the results may skip this section.

2.3.1 Formalism

The Lagrangian we will work with is

$$\mathcal{L}_{\text{quad}} = \frac{1}{2}\phi e^{-\square/M^2} (\square + \mu^2) \phi + \frac{1}{2}\gamma\phi^2 - \lambda\phi^4 \quad (2.3.1)$$

Here we have added a counter-term $\frac{1}{2}\gamma\phi^2$ with a coefficient γ which will be adjusted so that the value of the condensate in the vacuum is the same as the classical expression $\mu^2/4\lambda$. It also insures that no new poles are introduced into the propagator. As before we represent the field in the form

$$\phi = v(T) + \phi_f \quad (2.3.2)$$

where $v(T)$ is the equilibrium value of the condensate at temperature T and ϕ_f is the fluctuation around it whose average value is zero. After making this shift, and acknowledging that terms linear in ϕ_f will average to zero in the functional integral, the Lagrangian can be written as

$$\mathcal{L} = \mathcal{L}_{\text{quad}} + \mathcal{L}_{\text{int}} + \mathcal{L}_{\text{ct}} - V_{\text{cl}}(v) \quad (2.3.3)$$

where

$$\begin{aligned} \mathcal{L}_{\text{quad}} &= \frac{1}{2}\phi_f \left[e^{-\square/M^2} (\square + \mu^2) - 12\lambda v^2 - \delta m^2 \right] \phi_f \\ \mathcal{L}_{\text{int}} &= -4\lambda v \phi_f^3 - \lambda \phi_f^4 \\ \mathcal{L}_{\text{ct}} &= \frac{1}{2} (\delta m^2 + \gamma) \phi_f^2 \\ V_{\text{cl}}(v) &= -\frac{1}{2} (\mu^2 + \gamma) v^2 + \lambda v^4. \end{aligned} \quad (2.3.4)$$

An additional mass shift δm^2 has been added to the quadratic part of the action and then subtracted as a counter-term. The reason is that as the temperature increases the value of the condensate v decreases to zero at a critical T_c , and therefore at some

temperature below T_c the effective squared mass in the propagator becomes negative. This just means that we should do our calculations with the dressed propagator (or our best estimate of it) and not the mean field propagator. The value of δm^2 has to be determined at each temperature self-consistently just like v does. The $V_{\text{cl}}(v)$ is the contribution to the classical potential from the condensate field.

The Feynman rules corresponding to the above action are as follows. The dressed propagator \mathcal{D} in the imaginary time formalism is given by

$$\mathcal{D}^{-1} = e^{(\omega_n^2 + p^2)/M^2} (\omega_n^2 + p^2 - \mu^2) + 12\lambda v^2 + \delta m^2 \quad (2.3.5)$$

while the mean field propagator is given by

$$\bar{\mathcal{D}}^{-1} = e^{(\omega_n^2 + p^2)/M^2} (\omega_n^2 + p^2 - \mu^2) + 12\lambda v^2. \quad (2.3.6)$$

The thermodynamic potential is

$$\Omega = V_{\text{cl}}(v) - \frac{T}{V} \ln \left\{ \int [d\phi_f] \exp \left(\int_0^\beta d\tau \int_V d^3x [\mathcal{L}_{\text{quad}} + \mathcal{L}_{\text{int}} + \mathcal{L}_{\text{ct}}] \right) \right\} \quad (2.3.7)$$

where $\beta = 1/T$ and V is the volume. In a diagrammatic expansion the field ϕ_f is represented by a solid line. The vertices can easily be read off from the expressions above. The quartic interaction ϕ_f^4 has the vertex $-\lambda$ and the cubic interaction ϕ_f^3 has the vertex $-4\lambda v$. A cross or X represents the counter-term $-(\delta m^2 + \gamma)$.

The thermodynamic potential can be considered a function of the equilibrium condensate and a functional of the dressed propagator [41, 40].

$$\Omega = V_{\text{cl}}(v) - \frac{1}{2}T \sum_n \int \frac{d^3p}{(2\pi)^3} \left\{ \ln (T^2 \mathcal{D}) - \mathcal{D} \bar{\mathcal{D}}^{-1} + 1 \right\} + \sum_{l=2}^{\infty} \Omega_l(v, \mathcal{D}) \quad (2.3.8)$$

The Ω_l is the l -loop contribution to the potential. (A counter-term counts as one loop in this context.) Extremizing with respect to v removes tadpole diagrams, and extremizing with respect to \mathcal{D} removes one particle irreducible diagrams. In the same way one could remove two particle irreducible diagrams by introducing dressed vertices. The equations that determine the equilibrium solution are

$$\frac{\partial \Omega}{\partial v} = -(\mu^2 + \gamma)v + 4\lambda v^3 + 12\lambda v T \sum_n \int \frac{d^3p}{(2\pi)^3} \mathcal{D} + \sum_{l=2}^{\infty} \frac{\partial \Omega_l(v, \mathcal{D})}{\partial v} = 0 \quad (2.3.9)$$

and

$$\mathcal{D}^{-1} - \bar{\mathcal{D}}^{-1} = 2 \sum_{l=2}^{\infty} \frac{\delta\Omega_l(v, \mathcal{D})}{\delta\mathcal{D}} \quad (2.3.10)$$

the latter being the Schwinger-Dyson equation. Due to the functional derivative the difference of the inverse propagators is frequency and momentum dependent in general. Thus δm^2 should in principle be the self-energy $\Pi(\omega_n, p)$. However, in the approximations used in this paper a constant δm^2 will suffice. Terminating the expansion at two loops results in the diagrams displayed in Fig. 2. We would like to point out that all loop diagrams are UV finite on account of the exponential damping of the propagator, and they are IR finite except at a second order critical temperature where the mass vanishes (correlation length diverges).

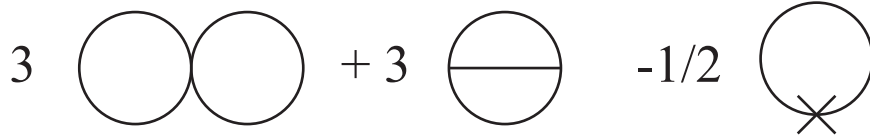


Figure 2.2: Two-loop contribution to $\ln Z$ including combinatoric factors and the counter-term.

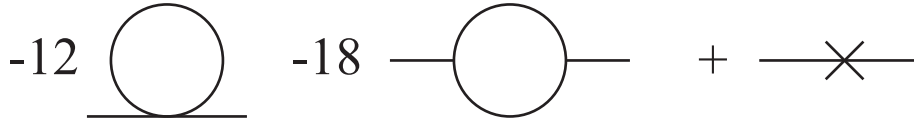


Figure 2.3: One loop contribution to the self-energy including combinatoric factors and the counter-term.

The behavior we expect is that the zero temperature condensate decreases with increasing temperature due to thermal fluctuations. If it goes to zero at a finite temperature T_c then a phase transition ought to have occurred. Now suppose that perturbation

theory can be applied, at least if we are not too close to T_c . To 1-loop order the equation for $v(T)$ is

$$v^2 = \frac{\mu^2 + \gamma}{4\lambda} - 3T \sum_n \int \frac{d^3p}{(2\pi)^3} \mathcal{D}. \quad (2.3.11)$$

The mass shift δm^2 can also be calculated. At 1-loop order it receives contributions from the diagrams shown in Fig. 3, which are obtained from those in Fig. 2. We will neglect the diagram involving the three point vertex; this will be justified *a posteriori*.

$$\delta m^2 = 12\lambda T \sum_n \int \frac{d^3p}{(2\pi)^3} \mathcal{D} - \gamma \quad (2.3.12)$$

Therefore, to 1-loop order

$$\delta m^2 = \mu^2 - 4\lambda v^2, \quad (2.3.13)$$

and the propagator to this order is

$$\mathcal{D}^{-1} = e^{(\omega_n^2 + p^2)/M^2} (\omega_n^2 + p^2 - \mu^2) + \mu^2 + 8\lambda v^2. \quad (2.3.14)$$

The temperature T_c where v goes to zero is the same temperature where the mass $\delta m^2 - \mu^2$ goes to zero.

The counter-term coefficient γ can readily be determined by calculating δm^2 at $T = 0$. In the $T \rightarrow 0$ limit

$$T \sum_n \rightarrow \int \frac{dp_4}{2\pi}$$

Under the assumption that $\mu \ll M$ the integral is trivial, and the requirement that $\delta m^2 = 0$ requires

$$\gamma = \frac{3\lambda M^2}{4\pi^2} \quad (2.3.15)$$

Working to higher order in the loop expansion would give the expansion of γ in a power series in λ .

Now let us consider the contribution of the 2-loop contributions to the thermodynamic potential. Referring to Fig. 2 they are

$$\Omega_{\text{quartic}} = 3\lambda \left[T \sum_n \int \frac{d^3p}{(2\pi)^3} \mathcal{D}(\omega_n, p) \right]^2 \quad (2.3.16)$$

and

$$\Omega_{\text{cubic}} = -48\lambda^2 v^2 T \sum_{n_1} \int \frac{d^3 p_1}{(2\pi)^3} T \sum_{n_2} \int \frac{d^3 p_2}{(2\pi)^3} \mathcal{D}(\omega_{n_1}, \mathbf{p}_1) \mathcal{D}(\omega_{n_2}, \mathbf{p}_2) \mathcal{D}(\omega_{n_1+n_2}, \mathbf{p}_1 + \mathbf{p}_2) \quad (2.3.17)$$

in an obvious notation. As emphasized before, the zero Matsubara mode dominates at high temperature, $T \gg M$, but still $T < T_c$ so that the cubic interaction does not vanish. (If it did then clearly $\Omega_{\text{cubic}} = 0$.) Hence

$$\Omega_{\text{quartic}} \sim \lambda M^2 T^2 \quad (2.3.18)$$

and

$$\Omega_{\text{cubic}} \sim \lambda^2 v^2 T^2 \ln(M^2/\lambda v^2) . \quad (2.3.19)$$

The diagram with the cubic vertices is smaller by a factor of $\lambda v^2/M^2$ which tends to zero at T_c even when including the logarithmic factor.

Similar conclusions can be reached for the self-energy. Using the dressed propagator of eq. (2.2.8) as reference we find that

$$\Pi_{\text{quartic}}(\omega_n, p) = 3\mu^2 - \frac{6\lambda MT}{\pi\sqrt{\pi}} \quad (2.3.20)$$

which is frequency and momentum independent and has the limit $2\mu^2$ at T_c . In contrast, at large frequency and momentum

$$\Pi_{\text{cubic}}(\omega_n, p) \sim \frac{\lambda^2 v^2 MT}{\omega_n^2 + p^2} \exp[-(\omega_n^2 + p^2)/M^2] \quad (2.3.21)$$

which is exponentially suppressed. At zero frequency and momentum

$$\Pi_{\text{cubic}}(0, 0) = -\frac{144\lambda^2 T^2}{\pi^2} \int_0^\infty \frac{dk k^2}{(k^2 + m_{\text{eff}}^2)^2} = -\frac{36\lambda^2 v^2 T}{\pi m_{\text{eff}}} = -\frac{9\sqrt{2}}{\pi} \lambda^{3/2} v T . \quad (2.3.22)$$

which goes to zero at T_c . This justifies the neglect of the diagrams involving the cubic interactions at high temperature.

Let us summarize the approximate expression for the thermodynamic potential. It includes the two loop diagram involving the four point vertex but not the two loop diagram involving the three point vertex; as argued previously, the latter is suppressed when $\lambda \ll 1$ and $\mu \ll M$.

$$\Omega = -\frac{1}{2} (\mu^2 + \gamma) v^2 + \lambda v^4 + \frac{1}{2} T \sum_n \int \frac{d^3 p}{(2\pi)^3} \ln(\beta^2 \mathcal{D}^{-1})$$

$$-\frac{1}{2}(\delta m^2 + \gamma) T \sum_n \int \frac{d^3 p}{(2\pi)^3} \mathcal{D} + 3\lambda \left[T \sum_n \int \frac{d^3 p}{(2\pi)^3} \mathcal{D} \right]^2 \quad (2.3.23)$$

The condensate satisfies

$$v^2 = \frac{\mu^2 + \gamma}{4\lambda} - 3T \sum_n \int \frac{d^3 p}{(2\pi)^3} \mathcal{D} \quad (2.3.24)$$

below T_c while $v = 0$ above T_c . The propagator is

$$\mathcal{D}^{-1} = e^{(\omega_n^2 + p^2)/M^2} (\omega_n^2 + p^2 - \mu^2) + \mu^2 + 8\lambda v^2 \quad (2.3.25)$$

below T_c and

$$\mathcal{D}^{-1} = e^{(\omega_n^2 + p^2)/M^2} (\omega_n^2 + p^2 - \mu^2) + \delta m^2 \quad (2.3.26)$$

above T_c , where

$$\delta m^2 = 12\lambda T \sum_n \int \frac{d^3 p}{(2\pi)^3} \mathcal{D} - \gamma. \quad (2.3.27)$$

It is useful to express the propagator as

$$\mathcal{D}^{-1}(\omega_n, p; m_{\text{eff}}^2) = e^{(\omega_n^2 + p^2)/M^2} (\omega_n^2 + p^2 - \mu^2) + \mu^2 + m_{\text{eff}}^2. \quad (2.3.28)$$

The quantity m_{eff} is approximately the pole mass when it is small compared to M . Rigorously speaking it is the screening mass. At zero temperature $m_{\text{eff}}^2 = 2\mu^2$ and is always non-negative, vanishing only at T_c . Below T_c we must solve for $v(T)$ self-consistently, and the result then also determines $m_{\text{eff}}(T)$. Above T_c we must solve for $\delta m^2(T)$ self-consistently, and this determines $m_{\text{eff}}(T)$.

2.3.2 Sums and Integrals

Let us calculate the relevant sums and integrals. We are interested in temperatures $T > \mu$ (previously, in section 2, we considered $T > M$) and mass scales $M > \mu$. Let us start with the oft-appearing quantity

$$T \sum_n \int \frac{d^3 p}{(2\pi)^3} \mathcal{D}.$$

Note that it is convergent in both the IR and UV. To the desired order

$$T \sum_n \int \frac{d^3 p}{(2\pi)^3} \mathcal{D} \approx T \sum_n \int \frac{d^3 p}{(2\pi)^3} \frac{e^{-(\omega_n^2 + p^2)/M^2}}{\omega_n^2 + p^2} \quad (2.3.29)$$

The trick is to use the integral representation

$$\sum_n \frac{e^{-(\omega_n^2+p^2)/M^2}}{\omega_n^2+p^2} = \frac{1}{M^2} \sum_n \int_1^\infty d\alpha^2 e^{-\alpha^2(\omega_n^2+p^2)/M^2} \quad (2.3.30)$$

and then use the function

$$\zeta(s) = \sum_{n=-\infty}^{\infty} e^{-s^2 n^2} \quad (2.3.31)$$

which appears so often in the study of the p -adic theory at finite temperature [32]. After integrating over momentum

$$T \sum_n \int \frac{d^3 p}{(2\pi)^3} \frac{e^{-(\omega_n^2+p^2)/M^2}}{\omega_n^2+p^2} = \frac{MT}{4\pi\sqrt{\pi}} f(T/M) \quad (2.3.32)$$

where we have defined the function

$$f(T/M) \equiv \int_1^\infty \frac{d\alpha}{\alpha^2} \zeta\left(\frac{2\pi T}{M}\alpha\right) \quad (2.3.33)$$

Therefore, to the desired accuracy

$$T \sum_n \int \frac{d^3 p}{(2\pi)^3} \mathcal{D} = \frac{MT}{4\pi\sqrt{\pi}} f(T/M). \quad (2.3.34)$$

The integral over α can be performed numerically, but it can also be calculated in the low and high temperature limits. These calculations are facilitated by an interesting property of the ζ function that

$$\zeta(s) = \frac{\sqrt{\pi}}{s} \zeta\left(\frac{\pi}{s}\right). \quad (2.3.35)$$

When $s > \sqrt{\pi}$

$$\zeta(s) = 1 + 2e^{-s^2} + 2e^{-4s^2} + \dots \quad (2.3.36)$$

and when $s < \sqrt{\pi}$

$$\zeta(s) = \frac{\sqrt{\pi}}{s} \left(1 + 2e^{-\pi^2/s^2} + 2e^{-4\pi^2/s^2} + \dots\right). \quad (2.3.37)$$

Using the above, we can calculate the behavior for $T \leq T_0$ and for $T \geq T_0$ where $T_0 \equiv M/2\sqrt{\pi}$. For $T \geq T_0$

$$f(T/M) = 1 + 2 \sum_{n=1}^{\infty} \left\{ e^{-4\pi^2 n^2 T^2/M^2} - \frac{2\pi\sqrt{\pi}nT}{M} \left[1 - \Phi\left(\frac{2\pi nT}{M}\right) \right] \right\} \quad (2.3.38)$$

where Φ is the probability integral

$$\Phi(u) = \frac{2}{\sqrt{\pi}} \int_0^u dt e^{-t^2}. \quad (2.3.39)$$

This has the high temperature expansion

$$f(T/M) = 1 + \frac{M^2}{4\pi^2 T^2} e^{-4\pi^2 T^2/M^2} + \mathcal{O}\left(\frac{M^4}{T^4} e^{-4\pi^2 T^2/M^2}\right). \quad (2.3.40)$$

For $T \leq T_0$ the integral can be broken up into two pieces, one from $\alpha = 1$ to $\alpha = \alpha_0$ and another from $\alpha = \alpha_0$ to $\alpha = \infty$, where $\alpha_0 = M/2\sqrt{\pi}T$.

$$f(T/M) = \frac{2\sqrt{\pi}T}{M} + \frac{M}{4\sqrt{\pi}T} \left(1 - \frac{4\pi T^2}{M^2}\right) + \frac{4\sqrt{\pi}T}{M} \sum_{n=1}^{\infty} \left[\frac{1}{2\pi n^2} \left(e^{-n^2\pi} - e^{-n^2 M^2/4T^2}\right) + e^{-n^2\pi} - n\pi (1 - \Phi(n\sqrt{\pi})) \right]. \quad (2.3.41)$$

The low temperature limit is

$$f(T/M) = \frac{M}{4\sqrt{\pi}T} + \frac{\pi\sqrt{\pi}}{3} \frac{T}{M} + \mathcal{O}\left(\frac{T}{M} e^{-M^2/4T^2}\right) \quad (2.3.42)$$

where we have used

$$1 + 2 \sum_{n=1}^{\infty} \left[\left(\frac{1}{\pi n^2} + 2\right) e^{-n^2\pi} - 2\pi n (1 - \Phi(n\sqrt{\pi})) \right] = \frac{\pi}{3} = 1.07163\dots \quad (2.3.43)$$

We have not proven the equality stated above, nor have we found reference to it in the literature, but it is true to any numerical accuracy that we have done.

Finally let us turn our attention to the one loop contribution

$$\frac{1}{2}T \sum_n \int \frac{d^3 p}{(2\pi)^3} \ln(\beta^2 \mathcal{D}^{-1}).$$

It can be expressed as

$$\frac{1}{2}T \sum_n \int \frac{d^3 p}{(2\pi)^3} \left\{ \int_0^{m_{\text{eff}}^2} \frac{d\alpha^2}{e^{(\omega_n^2 + p^2)/M^2} (\omega_n^2 + p^2 - \mu^2) + \mu^2 + \alpha^2} \right\} + \frac{1}{2}T \sum_n \int \frac{d^3 p}{(2\pi)^3} \ln \left[\beta^2 \left(e^{(\omega_n^2 + p^2)/M^2} (\omega_n^2 + p^2 - \mu^2) + \mu^2 \right) \right].$$

In the limit of small μ in comparison to M and T the second term can be written as

$$\frac{1}{2}T \sum_n \int \frac{d^3p}{(2\pi)^3} \left\{ \frac{\omega_n^2 + p^2}{M^2} + \ln [\beta^2(\omega_n^2 + p^2)] - \frac{\mu^2 [1 - e^{-(\omega_n^2 + p^2)/M^2}]}{\omega_n^2 + p^2} \right\} + \mathcal{O}(\mu^4)$$

The first term in curly brackets appears in the p -adic limit and it is zero [32]. The second term contributes one massless bosonic degree of freedom.

$$\frac{1}{2}T \sum_n \int \frac{d^3p}{(2\pi)^3} \ln [\beta^2(\omega_n^2 + p^2)] = -\frac{\pi^2}{90}T^4 + \text{vacuum} \quad (2.3.44)$$

The third term can be written as

$$\begin{aligned} & -\frac{1}{2}\mu^2 \int \frac{d^3p}{(2\pi)^3} \frac{1}{p} \frac{1}{e^{\beta p} - 1} - \frac{1}{2}\mu^2 \int \frac{d^4p}{(2\pi)^4} \frac{1}{p^2} + \frac{\mu^2 MT}{8\pi\sqrt{\pi}} f(T/M) \\ & = -\frac{\mu^2 T^2}{24} + \frac{\mu^2 MT}{8\pi\sqrt{\pi}} f(T/M) + \text{vacuum}. \end{aligned} \quad (2.3.45)$$

See [40] for the integrals. Hence, to the desired order

$$\frac{1}{2}T \sum_n \int \frac{d^3p}{(2\pi)^3} \ln (\beta^2 \mathcal{D}^{-1}(\omega_n, p; m_{\text{eff}})) = -\frac{\pi^2}{90}T^4 - \frac{\mu^2 T^2}{24} + \frac{m_{\text{eff}}^2 + \mu^2}{8\pi\sqrt{\pi}} MT f(T/M). \quad (2.3.46)$$

2.3.3 Equation of State for $M, T \gg \mu$

Now we assemble what we have learned in the limit that $M \gg \mu$ and $T \gg \mu$. The equation of state is expressed as pressure $P(T) = -\Omega(T)$ as a function of temperature T . The pressure is normalized to zero at zero temperature.

For $T \leq T_c$ the effective mass and condensate are given as functions of temperature by

$$m_{\text{eff}}^2 = 8\lambda v^2 = 2\mu^2 - \frac{3\lambda M^2}{2\pi^2} \left[4\sqrt{\pi} \frac{T}{M} f\left(\frac{T}{M}\right) - 1 \right] \quad (2.3.47)$$

The pressure is

$$P = \frac{\pi^2}{90}T^4 + \frac{\mu^2 T^2}{24} - \frac{3\mu^2 M^2}{32\pi^2} \left[4\sqrt{\pi} \frac{T}{M} f\left(\frac{T}{M}\right) - 1 \right] + \frac{3\lambda M^4}{128\pi^4} \left[4\sqrt{\pi} \frac{T}{M} f\left(\frac{T}{M}\right) - 1 \right]^2 \quad (2.3.48)$$

The entropy density $s(T) = dP(T)/dT$ can easily be computed by using the formula

$$T \frac{df(T/M)}{dT} = f(T/M) - \zeta(2\pi T/M) \quad (2.3.49)$$

It is

$$s(T) = \frac{2\pi^2}{45} T^3 + \frac{\mu^2 T}{12} +$$

$$\left[2f\left(\frac{T}{M}\right) - \zeta\left(\frac{2\pi T}{M}\right) \right] \left\{ \frac{3\lambda M^3}{16\pi^3 \sqrt{\pi}} \left[4\sqrt{\pi} \frac{T}{M} f\left(\frac{T}{M}\right) - 1 \right] - \frac{3\mu^2 M}{8\pi \sqrt{\pi}} \right\} \quad (2.3.50)$$

The energy density is $\epsilon(T) = -P(T) + Ts(T)$.

For $T \geq T_c$ the condensate is zero and the effective mass is determined by the formula

$$m_{\text{eff}}^2 = \frac{3\lambda M^2}{4\pi^2} \left[4\sqrt{\pi} \frac{T}{M} f\left(\frac{T}{M}\right) - 1 \right] - \mu^2 \quad (2.3.51)$$

The pressure is

$$P = \frac{\pi^2}{90} T^4 + \frac{\mu^2 T^2}{24} - \frac{3\lambda M^4}{256\pi^4} \left[4\sqrt{\pi} \frac{T}{M} f\left(\frac{T}{M}\right) - 1 \right]^2 - \frac{\mu^4}{16\lambda} \quad (2.3.52)$$

and the entropy density is

$$s(T) = \frac{2\pi^2}{45} T^3 + \frac{\mu^2 T}{12} - \frac{3\lambda M^3}{32\pi^3 \sqrt{\pi}} \left[2f\left(\frac{T}{M}\right) - \zeta\left(\frac{2\pi T}{M}\right) \right] \left[4\sqrt{\pi} \frac{T}{M} f\left(\frac{T}{M}\right) - 1 \right] \quad (2.3.53)$$

Both the condensate and the effective mass vanish at the critical temperature T_c determined by

$$\frac{T_c}{M} f\left(\frac{T_c}{M}\right) = \frac{1}{4\sqrt{\pi}} + \frac{\pi\sqrt{\pi}\mu^2}{3\lambda M^2} \quad (2.3.54)$$

At this temperature both the pressure

$$P(T_c) = \frac{\pi^2}{90} T_c^4 + \frac{\mu^2 T_c^2}{24} - \frac{\mu^4}{12\lambda} \quad (2.3.55)$$

and the entropy density

$$s(T_c) = \frac{2\pi^2}{45} T_c^3 + \frac{\mu^2 T_c}{12} + \frac{\mu^2 M}{8\pi \sqrt{\pi}} \left[\zeta\left(\frac{2\pi T_c}{M}\right) - 2f\left(\frac{T_c}{M}\right) \right] \quad (2.3.56)$$

are continuous, but the heat capacity $c_V(T) = Tds(T)/dT$ is not. Hence this is a second order phase transition.

2.4 Numerical Results and Comparison to Local Field Theory

The string motivated field theory under study has three parameters: M , μ and λ . What matters for the equation of state is not absolute magnitudes but relative magnitudes. The perturbative analysis we have used requires that $\lambda \ll 1$. However, since $\mu^2 > 0$ with the consequence of spontaneous symmetry breaking in the vacuum, the limit $\lambda = 0$ is not allowed since the theory would not be well-defined. We have assumed that the string scale M is large in comparison to the mass scale μ . We have also assumed that T is large compared to μ but made no assumption about the ratio T/M . From the point of view of conventional local field theory, M acts as an ultraviolet regulator. If one takes $M \rightarrow \infty$ in the action, one recovers the normal ϕ^4 field theory with spontaneous symmetry breaking. Let us examine the limits $T_c \ll M$ and $T_c \gg M$ analytically before turning to numerical calculations.

Suppose that $M \rightarrow \infty$ with μ^2/λ held fixed. Then it is easy to show that

$$m_{\text{eff}}^2(T) = \begin{cases} 2\mu^2 (1 - T^2/T_c^2) & \text{if } T \leq T_c \\ \mu^2 (T^2/T_c^2 - 1) & \text{if } T \geq T_c \end{cases} \quad (2.4.1)$$

with $T_c^2 = \mu^2/\lambda$. The condensate is determined by $8\lambda v^2(T) = m_{\text{eff}}^2(T)$ when $T \leq T_c$ while $v(T) = 0$ when $T \geq T_c$. The equation of state below T_c is

$$\begin{aligned} P(T) &= \left(\frac{\pi^2}{90} + \frac{\lambda}{24} \right) T^4 - \frac{\mu^2 T^2}{12} \\ s(T) &= 4 \left(\frac{\pi^2}{90} + \frac{\lambda}{24} \right) T^3 - \frac{\mu^2 T}{6} \\ \epsilon(T) &= 3 \left(\frac{\pi^2}{90} + \frac{\lambda}{24} \right) T^4 - \frac{\mu^2 T^2}{12} \\ c_V(T) &= 12 \left(\frac{\pi^2}{90} + \frac{\lambda}{24} \right) T^3 - \frac{\mu^2 T}{6} \end{aligned} \quad (2.4.2)$$

and above T_c is

$$\begin{aligned}
P(T) &= \left(\frac{\pi^2}{90} - \frac{\lambda}{48} \right) T^4 + \frac{\mu^2 T^2}{24} - \frac{\mu^4}{16\lambda} \\
s(T) &= 4 \left(\frac{\pi^2}{90} - \frac{\lambda}{48} \right) T^3 + \frac{\mu^2 T}{12} \\
\epsilon(T) &= 3 \left(\frac{\pi^2}{90} - \frac{\lambda}{48} \right) T^4 + \frac{\mu^2 T^2}{24} + \frac{\mu^4}{16\lambda} \\
c_V(T) &= 12 \left(\frac{\pi^2}{90} - \frac{\lambda}{48} \right) T^3 + \frac{\mu^2 T}{12}
\end{aligned} \tag{2.4.3}$$

(Corrections to these formulas for large but finite M are suppressed by the factor $\exp(-M^2/4T^2)$.) Clearly P , s , and ϵ are continuous at T_c but c_V is not. These are well-known, conventional finite temperature field theory results [40]. Because λ is required to be small, and $T \gg \mu$, the equation of state to first approximation is $\epsilon = 3P$. To focus on the effect of interactions, especially near T_c , it is useful to define the dimensionless interaction measure $(\epsilon - 3P)/\mu^2 T^2$. From the above

$$\frac{\epsilon - 3P}{\mu^2 T^2} = \begin{cases} \frac{1}{6} & \text{if } T \leq T_c \\ \frac{1}{4} \frac{T_c^2}{T^2} - \frac{1}{12} & \text{if } T \geq T_c \end{cases} \tag{2.4.4}$$

Obviously it is continuous at T_c but its derivative is not.

Now suppose that $\lambda M^2 \ll \mu^2$. Then $T_c \gg M$ and so we focus on temperatures such that $T \gg M$. In this case,

$$m_{\text{eff}}^2(T) = \begin{cases} 2\mu^2 (1 - T/T_c) & \text{if } T \leq T_c \\ \mu^2 (T/T_c - 1) & \text{if } T \geq T_c \end{cases} \tag{2.4.5}$$

with $T_c = \pi\sqrt{\pi}\mu^2/3\lambda M$. The condensate is determined by $8\lambda v^2(T) = m_{\text{eff}}^2(T)$ when $T \leq T_c$ while $v(T) = 0$ when $T \geq T_c$. The equation of state below T_c is

$$\begin{aligned}
P(T) &= \frac{\pi^2}{90} T^4 + \left(\frac{\mu^2}{24} + \frac{3\lambda M^2}{8\pi^3} \right) T^2 - \frac{3\mu^2 M T}{8\pi\sqrt{\pi}} \\
s(T) &= 4 \frac{\pi^2}{90} T^3 + 2 \left(\frac{\mu^2}{24} + \frac{3\lambda M^2}{8\pi^3} \right) T - \frac{3\mu^2 M}{8\pi\sqrt{\pi}} \\
\epsilon(T) &= 3 \frac{\pi^2}{90} T^4 + \left(\frac{\mu^2}{24} + \frac{3\lambda M^2}{8\pi^3} \right) T^2 \\
c_V(T) &= 12 \frac{\pi^2}{90} T^3 + 2 \left(\frac{\mu^2}{24} + \frac{3\lambda M^2}{8\pi^3} \right) T
\end{aligned} \tag{2.4.6}$$

and above T_c is

$$\begin{aligned}
P(T) &= \frac{\pi^2}{90}T^4 + \left(\frac{\mu^2}{24} - \frac{3\lambda M^2}{16\pi^3}\right)T^2 - \frac{\mu^4}{16\lambda} \\
s(T) &= 4\frac{\pi^2}{90}T^3 + 2\left(\frac{\mu^2}{24} - \frac{3\lambda M^2}{16\pi^3}\right)T \\
\epsilon(T) &= 3\frac{\pi^2}{90}T^4 + \left(\frac{\mu^2}{24} - \frac{3\lambda M^2}{16\pi^3}\right)T^2 + \frac{\mu^4}{16\lambda} \\
c_V(T) &= 12\frac{\pi^2}{90}T^3 + 2\left(\frac{\mu^2}{24} - \frac{3\lambda M^2}{16\pi^3}\right)T
\end{aligned} \tag{2.4.7}$$

(Corrections to these formulas are suppressed by the factor $\exp(-4\pi^2 T^2/M^2)$.) Once again, P , s , and ϵ are continuous at T_c but c_V is not. The most noticeable difference is that in the conventional local field theory the effective mass-squared vanishes as $|T^2 - T_c^2|$, whereas for the string field theory it vanishes as $|T - T_c|$, although the difference is inconsequential in the limit $T \rightarrow T_c$. The difference in the exponents is seen in the interaction measure too.

$$\frac{\epsilon - 3P}{\mu^2 T^2} = \begin{cases} -\frac{1}{12} + \frac{M}{8\pi\sqrt{\pi}T_c} \left(9\frac{T_c}{T} - 2\right) & \text{if } T \leq T_c \\ -\frac{1}{12} + \frac{M}{8\pi\sqrt{\pi}T_c} \left(6\frac{T_c^2}{T^2} + 1\right) & \text{if } T \geq T_c \end{cases} \tag{2.4.8}$$

Of course, our calculation is basically a mean-field approximation so the values of critical exponents cannot be taken as being very accurate.

It is instructive to examine the dependence of the discontinuity in the specific heat at the critical temperature as a function of T_c/M to see the transition from conventional local field theory ($T_c/M \ll 1$) to the ‘‘SFT’’ limit ($T_c/M \gg 1$). In those two limits the discontinuity can be calculated analytically.

$$c_V(T_{c-}) - c_V(T_{c+}) = \lambda T_c^3 \begin{cases} \frac{1}{2} & \text{if } T_c \ll M \\ \frac{9}{8\pi^3} \left(\frac{M}{T_c}\right)^2 & \text{if } T_c \gg M \end{cases} \tag{2.4.9}$$

The discontinuity decreases monotonically with increasing T_c/M when measured in units of λT_c^3 , the only sensible unit for comparison.

Now we show some full numerical results which do not make any assumption about the magnitude of T_c/M . Figure 4 shows the dependence of T_c/M on the variable

$\mu^2/\lambda M^2$. It changes from the square-root to linear dependence very rapidly when $T_c/M \sim 0.4$. Figure 5 shows the dependence of $m_{\text{eff}}^2/2\mu^2$ on T/T_c for a value of $T_c/M \ll 1$ and for a value $T_c/M \gg 1$. The figure clearly shows the quadratic dependence for small T_c/M versus the linear dependence for large T_c/M . Figure 6 shows the interaction measure, or deviation from the ideal relativistic equation of state $\epsilon = 3P$, for both small and large values of T_c/M . Finally, Fig. 7 shows the discontinuity in the heat capacity at the critical temperature as a function of T_c/M ; it decreases monotonically towards zero as $T_c/M \rightarrow \infty$.

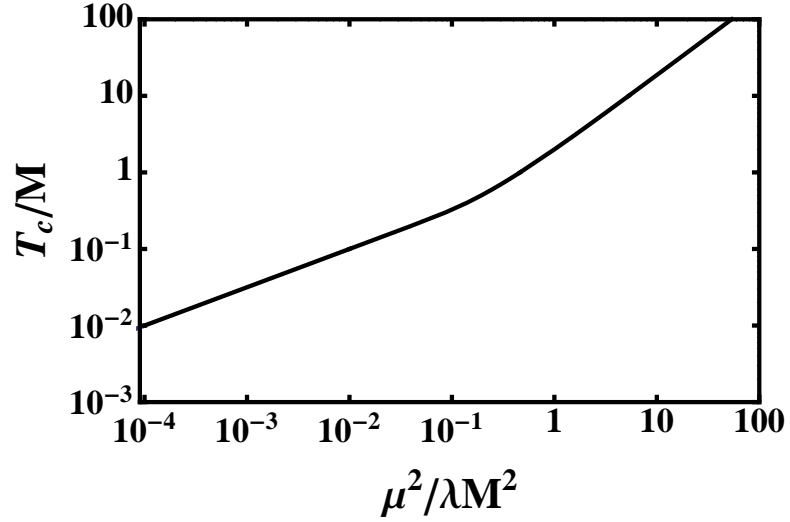


Figure 2.4: Scaling of the critical temperature with the parameters. The dependence changes from square-root to linear around $T_c/M \sim 0.4$.

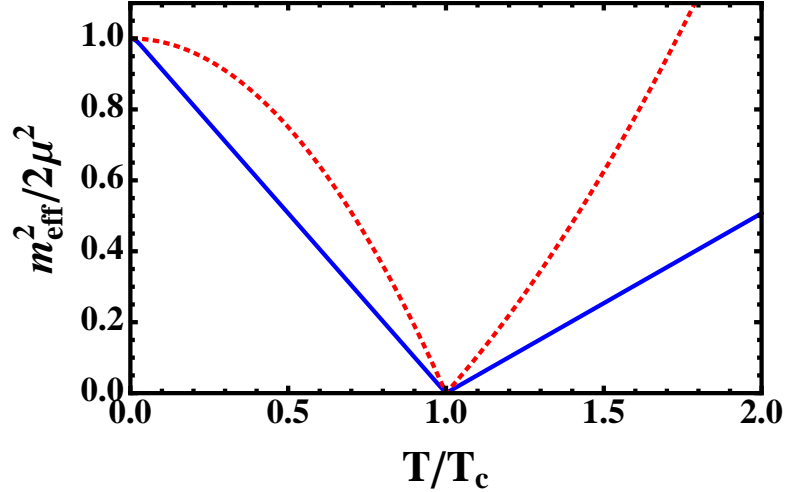


Figure 2.5: Dependence of the effective mass on temperature for $T_c/M = 1/100$ (dashed/red) and $T_c/M = 10$ (solid/blue).

2.5 Effective Potential

For a given temperature the field ϕ has a stable equilibrium value $v(T)$, as discussed and computed in previous sections. If for some reason the average deviates from its thermal value by an amount ξ , there will be a restoring force. This restoring force is described by an effective potential $U(\xi)$. In essence, this is an expansion away from equilibrium states. It is useful in many areas of physics, including statistical physics, particle physics, and cosmology. In this section we compute the first few terms in the expansion at the 1-loop order.

Let us define

$$\phi = \bar{\phi} + \phi_f \quad (2.5.1)$$

where $\bar{\phi}$ is a constant field and ϕ_f is the fluctuation around it whose average value is zero. Let us further write

$$\bar{\phi} = v(T) + \xi. \quad (2.5.2)$$

Here $v(T)$ is the equilibrium value of the condensate at temperature T which was previously determined. The ξ is a space and time independent (or slowly varying on all

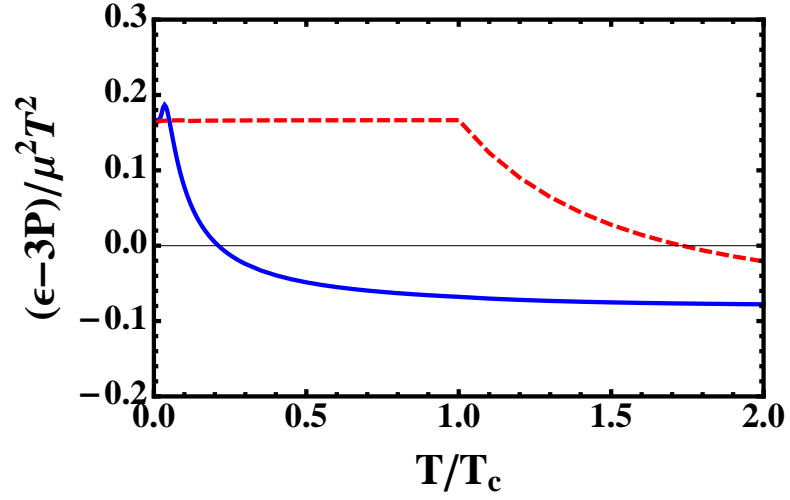


Figure 2.6: The interaction measure as a function of temperature for $T_c/M = 1/100$ (dashed/red) and $T_c/M = 10$ (solid/blue).

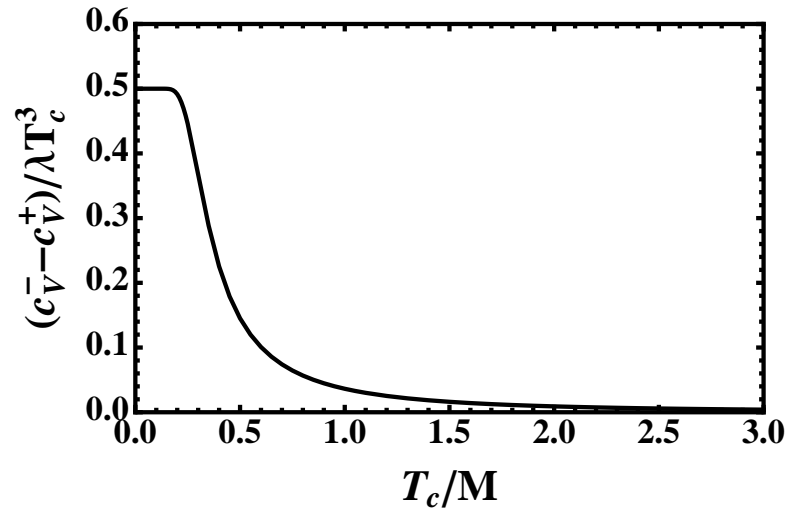


Figure 2.7: Discontinuity in the heat capacity at the critical temperature.

natural length and time scales) deviation from the equilibrium value that we take as a parameter to be varied at will. We will calculate deviations from the thermodynamic potential at each temperature as a function of ξ ; this is the effective potential (commonly referred to as the effective action in particle physics). The Lagrangian can be written as

$$\mathcal{L} = \mathcal{L}_{\text{quad}} + \mathcal{L}_{\text{int}} + \mathcal{L}_{\text{ct}} - V_{\text{cl}}(v) - U_{\text{cl}}(\xi) - V_{\xi}(\phi_f) \quad (2.5.3)$$

where

$$\begin{aligned} \mathcal{L}_{\text{quad}} &= \frac{1}{2}\phi_f \left[e^{-\square/M^2} (\square + \mu^2) - 12\lambda v^2 - \delta m^2 \right] \phi_f \\ \mathcal{L}_{\text{int}} &= -4\lambda v \phi_f^3 - \lambda \phi_f^4 \\ \mathcal{L}_{\text{ct}} &= \frac{1}{2} (\delta m^2 + \gamma) \phi_f^2 \\ V_{\text{cl}}(v) &= -\frac{1}{2} (\mu^2 + \gamma) v^2 + \lambda v^4 \\ U_{\text{cl}}(\xi) &= (4\lambda v^2 - \mu^2 - \gamma) v \xi + \frac{1}{2} (12\lambda v^2 - \mu^2 - \gamma) \xi^2 + 4\lambda v \xi^3 + \lambda \xi^4 \\ V_{\xi}(\phi_f) &= 6\lambda (2v\xi + \xi^2) \phi_f^2 + 4\lambda \xi \phi_f^3. \end{aligned} \quad (2.5.4)$$

The first four terms in the Lagrangian were already introduced and used previously. The last two terms vanish when $\xi = 0$. The $U_{\text{cl}}(\xi)$ is the contribution to the classical potential from the ξ field. The $V_{\xi}(\phi_f)$ gives the interaction between the deviational field ξ and the quantum field ϕ_f ; it will be used to determine the effective potential at a given temperature.

The Feynman rules corresponding to the above action are the same as before but with additional terms arising from the presence of ξ . The thermodynamic potential is now

$$\Omega = V_{\text{cl}}(v) + U_{\text{cl}}(\xi) - \frac{T}{V} \ln \left\{ \int [d\phi_f] \exp \left(\int_0^\beta d\tau \int_V d^3x [\mathcal{L}_{\text{quad}} + \mathcal{L}_{\text{int}} + \mathcal{L}_{\text{ct}} - V_{\xi}] \right) \right\} \quad (2.5.5)$$

In a diagrammatic expansion the field ϕ_f is represented by a solid line while the external field ξ is represented by a wavy line. The vertices can easily be read off from the expressions above. For example, the quartic interaction ϕ_f^4 has the vertex $-\lambda$, the cubic interaction ϕ_f^3 has the vertex $-4\lambda v$, and the cubic interaction $\xi \phi_f^2$ has the vertex $-12\lambda v$.

Now let us extrapolate away from the equilibrium value of the condensate so that ξ is not equal to zero. The effective potential for ξ is

$$U(\xi) = U_{\text{cl}}(\xi) + U_{\text{loop}}(\xi) \quad (2.5.6)$$

where

$$U_{\text{loop}}(\xi) = -\frac{T}{V} \ln \left\{ \frac{\int [d\phi_f] e^S e^{-\int d\tau d^3x V_\xi(\phi_f)}}{\int [d\phi_f] e^S} \right\}. \quad (2.5.7)$$

Here S is the action due to $\mathcal{L}_{\text{quad}} + \mathcal{L}_{\text{int}} + \mathcal{L}_{\text{ct}}$. This can be expanding in an infinite series in ξ . The effective potential has the property that $U(0) = 0$.

It is straightforward to compute the 1-loop contribution to U to all orders in ξ . Expand the exponential of V_ξ to the N_1 'th order in $\xi\phi_f^2$ and to the N_2 'th order in $\xi^2\phi_f^2$; the term $\xi\phi_f^3$ cannot contribute to the one loop order. Expansion of the exponential gives rise to a factor $1/(N_1!N_2!)$. Each of these $N_1 + N_2$ terms has two ϕ_f legs. These must be connected to make one and only one loop. The ordering does not matter. Taking into account the vertices, this leads to

$$-\frac{(N_1 + N_2 - 1)!}{2N_1!N_2!} (-24\lambda v\xi)^{N_1} (-12\lambda\xi^2)^{N_2} T \sum_n \int \frac{d^3p}{(2\pi)^3} \mathcal{D}^{N_1+N_2} \quad (2.5.8)$$

Summing over all N_1 and N_2 gives $U_{1\text{-loop}}(\xi)$ with the obvious requirement that $N_1 + N_2 > 0$. When summed with $U_{\text{cl}}(\xi)$ the term linear in ξ should vanish, otherwise we would not be at the extremum of Ω . This term is

$$(4\lambda v^2 - \mu^2 - \gamma) v\xi + 12\lambda v\xi T \sum_n \int \frac{d^3p}{(2\pi)^3} \mathcal{D}$$

which does vanish on account of the equation satisfied by v at one loop order.

Let us examine $U_{\text{loop}}(\xi)$ when $T > T_c$. Since $v(T) = 0$ there are no three point vertices.

$$U_{\text{loop}}(\xi, T) = 6\lambda\xi^2 T \sum_n \int \frac{d^3p}{(2\pi)^3} \mathcal{D} + \frac{1}{2}T \sum_n \int \frac{d^3p}{(2\pi)^3} \sum_{N=2}^{\infty} \frac{(-1)^{N+1}}{N} (12\lambda\xi^2)^N \mathcal{D}^N \quad (2.5.9)$$

The reason for separating out the term quadratic in ξ is that it naturally combines with the quadratic piece in U_{cl} to yield $\frac{1}{2}m_{\text{eff}}^2\xi^2$. The remaining terms can be exactly summed; they are referred to as the ring diagrams [40].

$$U_{\text{ring}}(\xi, T) = \frac{1}{2}T \sum_n \int \frac{d^3p}{(2\pi)^3} [\ln(1 + 12\lambda\xi^2\mathcal{D}) - 12\lambda\xi^2\mathcal{D}] \quad (2.5.10)$$

The propagator is

$$\mathcal{D}^{-1} = e^{(\omega_n^2 + p^2)/M^2} (\omega_n^2 + p^2 - \mu^2) + m_{\text{eff}}^2 + \mu^2. \quad (2.5.11)$$

The sum and integral in U_{ring} are dominated by $n = 0$ and $p \rightarrow 0$, respectively, because there is no need for a UV cut-off in (2.5.9) for $N \geq 2$. The result is

$$\begin{aligned} U_{\text{ring}}(\xi, T) &= \frac{1}{2}T \int \frac{d^3p}{(2\pi)^3} \left[\ln \left(1 + \frac{12\lambda\xi^2}{p^2 + m_{\text{eff}}^2} \right) - \frac{12\lambda\xi^2}{p^2 + m_{\text{eff}}^2} \right] \\ &= -\frac{T}{12\pi} \left[(m_{\text{eff}}^2 + 12\lambda\xi^2)^{3/2} - m_{\text{eff}}^3 - 18\lambda m_{\text{eff}}\xi^2 \right]. \end{aligned} \quad (2.5.12)$$

Thus the potential for $T > T_c$ is

$$U(\xi, T) = \frac{1}{2}m_{\text{eff}}^2(T)\xi^2 + \lambda\xi^4 + U_{\text{ring}}(\xi, T) + \dots \quad (2.5.13)$$

One must be careful about using this expression too close to T_c where fluctuations are large and where critical phenomena occur (nonanalytic critical exponents etc.). It is only valid when $\xi^2 < m_{\text{eff}}^2/12\lambda$ because otherwise the series does not converge to a logarithm. This region shrinks to zero as T_c is approached from above.

When $T < T_c$ a double series must be summed. In this case we write

$$U_{\text{loop}}(\xi, T) = 6\lambda(2v\xi + \xi^2)T \sum_n \int \frac{d^3p}{(2\pi)^3} \mathcal{D} + U_{\text{ring}}(\xi, T) \quad (2.5.14)$$

where

$$\begin{aligned} U_{\text{ring}}(\xi, T) &= -\frac{1}{2}T \sum_n \int \frac{d^3p}{(2\pi)^3} \left[\sum_{N_1=1}^{\infty} \sum_{N_2=1}^{\infty} \frac{(N_1 + N_2 - 1)!}{N_1!N_2!} (-x)^{N_1} (-y)^{N_2} \right. \\ &\quad \left. + \sum_{N_1=1}^{\infty} \frac{(-x)^{N_1}}{N_1} + \sum_{N_2=1}^{\infty} \frac{(-y)^{N_2}}{N_2} + x + y \right] \end{aligned} \quad (2.5.15)$$

and where $x = 24\lambda v\xi\mathcal{D}$ and $y = 12\lambda\xi^2\mathcal{D}$. By using the integral representation

$$(N_1 + N_2 - 1)! = \int_0^{\infty} dt e^{-t} t^{N_1+N_2-1} \quad (2.5.16)$$

the sums can be done followed by integration over t with the result that

$$U_{\text{ring}}(\xi, T) = \frac{1}{2}T \sum_n \int \frac{d^3p}{(2\pi)^3} [\ln(1 + x + y) - x - y]. \quad (2.5.17)$$

As before, the sum and integral in U_{ring} are dominated by $n = 0$ and $p \rightarrow 0$, with the result that

$$U_{\text{ring}}(\xi, T) = -\frac{T}{12\pi} \left[(m_{\text{eff}}^2 + 24\lambda v\xi + 12\lambda\xi^2)^{3/2} - m_{\text{eff}}^3 - \frac{3}{2}m_{\text{eff}}(24\lambda v\xi + 12\lambda\xi^2) \right]. \quad (2.5.18)$$

Thus the potential for $T < T_c$, including both the classical and one loop contributions, is

$$U(\xi, T) = \frac{1}{2}m_{\text{eff}}^2(T)\xi^2 + 4\lambda v\xi^3 + \lambda\xi^4 + U_{\text{ring}}(\xi, T) + \dots \quad (2.5.19)$$

This expression makes use of the solution for $v(T)$. Previous caution concerning the radius of convergence in ξ apply here as well.

Both the $T < T_c$ and $T > T_c$ potentials have the property that

$$m_{\text{eff}}^2(T) = \frac{\partial^2 U(\xi = 0, T)}{\partial \xi^2}$$

which is an oft-cited relationship. However, it is only true when the self-energy is frequency and momentum independent. The astute reader will notice that there is a contribution of order ξ^2 coming from U_{ring} when $T < T_c$ (but not when $T > T_c$). This contribution is of order $\lambda^{3/2}$ and therefore is subleading in an expansion in λ . The magnitude and sign of this contribution is exactly that arising from the one loop self-energy diagram with cubic vertices, evaluated in the zero frequency and zero momentum limit; see eq. (2.3.22).

$$\frac{\partial^2 U_{\text{ring}}(\xi = 0)}{\partial \xi^2} = \Pi_{\text{cubic}}(0, 0) \quad (2.5.20)$$

We have already decided to drop such subleading terms. For further discussion on this point see [42, 40]

It should be apparent that the results of this section are independent of whether the underlying action is the string field theory or the conventional local field theory. The differences only appear when explicit functions of $m_{\text{eff}}(T)$ and $v(T)$ are used along with the relationship of T_c to the parameters in the action. For example, when $T_c \ll M$ (and dropping the ring contribution)

$$\frac{U}{\mu^2 T_c^2} = \begin{cases} \frac{1}{2} \frac{m_{\text{eff}}^2}{\mu^2} \left(\frac{\xi}{T_c} \right)^2 + \sqrt{2} \frac{m_{\text{eff}}}{\mu} \left(\frac{\xi}{T_c} \right)^3 + \left(\frac{\xi}{T_c} \right)^4 & \text{if } T \leq T_c \\ \frac{1}{2} \frac{m_{\text{eff}}^2}{\mu^2} \left(\frac{\xi}{T_c} \right)^2 + \left(\frac{\xi}{T_c} \right)^4 & \text{if } T \geq T_c \end{cases} \quad (2.5.21)$$

and when $T_c \gg M$ (again dropping the ring contribution)

$$\frac{U}{\mu^2 T_c^2} = \begin{cases} \frac{1}{2} \frac{m_{\text{eff}}^2}{\mu^2} \left(\frac{\xi}{T_c}\right)^2 + \sqrt{\frac{2\pi\sqrt{\pi}}{3}} \frac{T_c}{M} \frac{m_{\text{eff}}}{\mu} \left(\frac{\xi}{T_c}\right)^3 + \frac{\pi\sqrt{\pi}}{3} \frac{T_c}{M} \left(\frac{\xi}{T_c}\right)^4 & \text{if } T \leq T_c \\ \frac{1}{2} \frac{m_{\text{eff}}^2}{\mu^2} \left(\frac{\xi}{T_c}\right)^2 + \frac{\pi\sqrt{\pi}}{3} \frac{T_c}{M} \left(\frac{\xi}{T_c}\right)^4 & \text{if } T \geq T_c \end{cases} \quad (2.5.22)$$

As examples, we show the effective potential (without the ring contribution) in Figs. 8 and 9 for $T_c/M = 1/100$ and $T_c/M = 10$, respectively, for T below, at, and above the critical temperature.

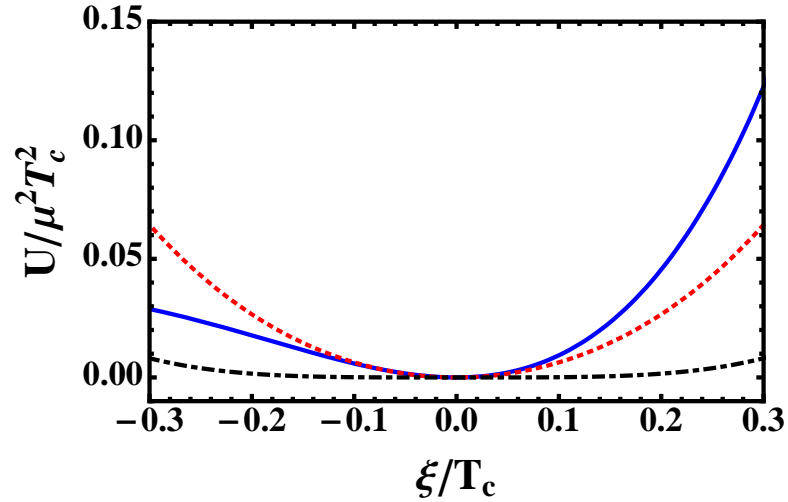


Figure 2.8: Effective potential for $T_c/M = 1/100$ at $T/T_c=0.5$ (solid/blue), 1.0 (dash-dotted/black), and 1.5 (dashed/red).

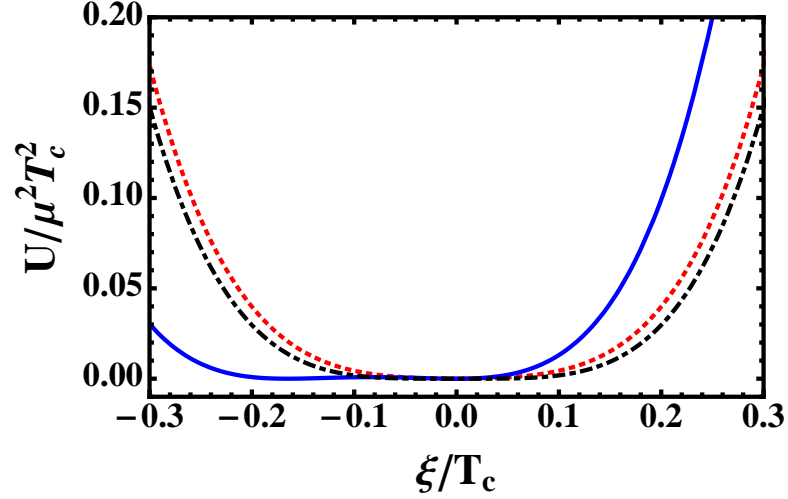


Figure 2.9: Effective potential for $T_c/M = 10$ at $T/T_c=0.5$ (solid/blue), 1.0 (dash-dotted/black), and 1.5 (dashed/red).

2.6 Conclusion

We investigated the thermodynamic properties of a tachyon with a string field theory motivated nonlocal action. We first studied the phase transition in the high temperature limit to 1-loop order. We introduced the mass shift δm^2 and calculated the thermodynamic potential around the temperature dependent true minimum, $v(T)$. We found that at the 1-loop level both the mass shift, δm^2 , and the minimum, $v(T)$, go to zero at the same critical temperature which strongly indicates a second order phase transition.

We then performed a more involved analysis. Here we included a counter-term to allow us to make a comparison to the conventional ϕ^4 theory. We calculated the equation of state to 2-loop order. We argued that the cubic contribution is suppressed compared to the quartic near the critical temperature. We were able to analytically calculate the equation of state and hence the thermodynamic quantities in the limit $T, M > \mu$. As expected, we found that at the critical temperature both the pressure and the entropy density were continuous but the heat capacity was not, signaling a second order phase transition. The discontinuity in the heat capacity, in natural units of λT_c^3 , was found

to decrease monotonically with T_c/M .

Checking the consistency of our analysis, we made the comparison with ordinary local field theory by taking the limit that the string parameter $M \rightarrow \infty$. Doing so we recovered the usual local field theory result. We compared this with analytical approximations of our thermodynamic quantities for finite M . We also calculated the interaction measure for both cases. Aside from the M dependence of the thermodynamic quantities in the string case, we found that the effective mass-squared vanished as $|T - T_c|$ compared to $|T^2 - T_c^2|$ in the conventional case.

In the last section we included the possibility of the the field being out of equilibrium at temperature T by a small amount and computed the corresponding effective potential. This allowed us to compute the finite temperature effective potential. We found that we were able to calculate the 1-loop contribution to the effective potential at all orders in ξ for temperature both above and below T_c . For both cases the ring contribution is only valid for $\xi^2 < m_{eff}^2/12\lambda$. It was also seen that both potentials satisfy the usual relationship $m_{\text{eff}}^2(T) = \partial^2 U(\xi = 0, T)/\partial \xi^2$.

We were able to calculate results that were consistent with conventional scalar field theory in the relevant limit. In the limit investigated, $T, M > \mu$, we found that this nonlocal theory is very similar to the conventional one, but we were able to see effects from the stringy nonlocality. The formalism developed in this paper will help us explore the more challenging, but perhaps more interesting, case when $M \sim \mu$. Our calculations may also be relevant for capturing the thermal properties of the Early Universe which is relevant for some cosmological models .

Chapter 3

Review of Nuclear Matter

3.1 Introduction

The study of nuclear matter would most fundamentally require the study of quantum chromodynamics. While QCD is the formal theory describing the strong interaction, due to this strong coupling we cannot use the usual methods of perturbation theory. However, at energies relevant to most nuclear properties, we are able to study some of these phenomena by the use of effective field theories. In these effective field theories, hadrons become the degrees of freedom rather than quarks and gluons. More specifically, we can describe the interaction of nucleons via mesons. Quantum Hydrodynamics, the traditional model of nucleon-nucleon interaction which can be used to describe bulk nuclear matter was given by Walecka[43]. It contains neutrons and protons whose interactions are mediated by the exchange of the electrically neutral scalar σ and vector ω mesons. At the mean field level it is relatively simple and provides a fit to many properties of nuclear matter.

In the static nonrelativistic limit the effective nucleon-nucleon potential becomes the Yukawa potential. If we choose the constants appropriately we see that the potential is repulsive at short distances and attractive at long distances which is the needed behavior for a description of nuclear matter.

$$V(r) = \frac{g_\omega^2}{4\pi} \frac{e^{-m_\omega r}}{r} - \frac{g_\sigma^2}{4\pi} \frac{e^{-m_\sigma r}}{r} \quad (3.1.1)$$

The Lagrangian for containing these interactions is given by

$$\mathcal{L}_W = \bar{\psi} [i\cancel{\partial} - g_\omega\psi - M + g_\sigma\sigma] \psi - \frac{1}{2}m_\sigma^2\sigma^2 + \frac{1}{2}m_\omega^2\omega^2 - \frac{1}{4}F^{\mu\nu}F_{\mu\nu} + \frac{1}{2}m_\omega^2\omega_\mu\omega^\mu \quad (3.1.2)$$

where

$$F_{\mu\nu} = \partial_\mu\omega_\nu - \partial_\nu\omega_\mu \quad (3.1.3)$$

3.2 Walecka Model

Given the Lagrangian for our effective theory we can now make use of the methods of finite temperature field theory. The general partition function is given by

$$Z = \int [d\bar{\psi}_p][d\psi_p][d\bar{\psi}_n][d\psi_n][d\sigma][d\omega_\mu] \exp\left(\int_0^\beta d\tau \int d^3x (\mathcal{L}_W + \mu_p\psi_p^\dagger\psi_p + \mu_n\psi_n^\dagger\psi_n)\right) \quad (3.2.4)$$

However, as mentioned before, we will start by considering symmetric nuclear matter. Since this is the case, we can set $\mu = \mu_n = \mu_p$. Lagrange's equations give the field equations

$$(\partial^2 + m_\sigma^2)\sigma = g_\sigma\bar{\psi}\psi \quad (3.2.5)$$

$$\partial_\mu F^{\mu\nu} + m_\omega^2\omega^\nu = g_\omega\bar{\psi}\gamma^\nu\psi \quad (3.2.6)$$

From this we see that the nucleons act as source terms. So, when the nucleon density is nonzero we would have nonzero expectation values for the σ and ω fields. One way to examine this is to replace by its expectation value plus fluctuations. This gives

$$\sigma = \bar{\sigma} + \sigma' \quad (3.2.7)$$

$$\omega_\mu = \delta_{\mu 0}\bar{\omega}_0 + \omega'_\mu \quad (3.2.8)$$

For a static, uniform system, $\bar{\omega}_i = 0$ on account of rotational symmetry. In the mean field approximation we neglect the fluctuations so the fields are replaced with their

average values. Doing this, the partition function becomes

$$Z = \int [d\bar{\psi}_p][d\psi_p][d\bar{\psi}_n][d\psi_n][d\sigma][d\omega_\mu] \\ \times \exp \left(\int_0^\beta d\tau \int d^3x (\bar{\psi}[i\cancel{D} - (M - g_\sigma\bar{\sigma}) + (\mu - g_\omega\bar{\omega}_0)\gamma_0]\psi - \frac{1}{2}m_\sigma^2 + \frac{1}{2}m_\omega^2\bar{\omega}_0^2) \right) \quad (3.2.9)$$

We see that we have the usual partition function for a Fermi gas, except that it now has an effective mass given by

$$M^* = M - g_\sigma\bar{\sigma} \quad (3.2.10)$$

as well as an effective chemical potential.

$$\mu^* = \mu - g_\omega\bar{\omega}_0 \quad (3.2.11)$$

Using this observation, we can now write down the pressure and the energy in the mean field approximation as follows

$$P = P_{FG} - \frac{1}{2}m_\sigma^2\bar{\sigma}^2 + \frac{1}{2}m_\omega^2\bar{\omega}_0^2 \quad (3.2.12)$$

$$\mathcal{E} = \mathcal{E}_{FG} + \frac{1}{2}m_\sigma^2\bar{\sigma}^2 + \frac{1}{2}m_\omega^2\bar{\omega}_0^2 \quad (3.2.13)$$

To determine the value of the mean fields we can extremeize the pressure with respect to each field. Doing so we find

$$\bar{\sigma} = - \left(\frac{g_\sigma}{m_\sigma^2} \right) \frac{\partial P_{FG}}{\partial M^*} = \frac{g_\sigma}{m_\sigma^2} \rho_s \quad (3.2.14)$$

$$\bar{\omega}_0 = \left(\frac{g_\omega}{m_\omega^2} \right) \frac{\partial P_{FG}}{\partial \mu^*} = \frac{g_\omega}{m_\omega^2} \rho_B \quad (3.2.15)$$

where

$$\rho_B = \frac{\gamma}{(2\pi)^3} \int_0^{k_F} d^3k = \frac{\gamma}{6\pi^2} k_F^3 \quad (3.2.16)$$

$$\rho_s = \frac{\gamma}{(2\pi)^3} \int_0^{k_F} d^3k \frac{M^*}{(k^2 + M^{*2})^{1/2}} \quad (3.2.17)$$

Here γ is the spin-isospin degeneracy which has a value of 4 for nuclear matter and 2 for pure neutron matter. The values of the mean fields can also be found from the field

equations in 3.5 and 3.6. Examining them under our assumptions of a static uniform system, we see that we find the same thing. We can now write the pressure and energy in terms of the effective mass which is determined self consistently.

$$P = \frac{g_\omega^2}{2m_\omega^2} \rho_B^2 - \frac{m_\sigma^2}{2g_\sigma^2} (M - M^*)^2 + \frac{1}{3} \frac{\gamma}{(2\pi)^3} \int_0^{k_F} d^3k \frac{M^*}{(k^2 + M^{*2})^{1/2}} \quad (3.2.18)$$

$$\mathcal{E} = \frac{g_\omega^2}{2m_\omega^2} \rho_B^2 + \frac{m_\sigma^2}{2g_\sigma^2} (M - M^*)^2 + \frac{\gamma}{(2\pi)^3} \int_0^{k_F} d^3k (k^2 + M^{*2})^{1/2} \quad (3.2.19)$$

$$M^* = M - \frac{g_\sigma^2}{m_\sigma^2} \frac{\gamma}{(2\pi)^3} \int_0^{k_F} d^3k \frac{M^*}{(k^2 + M^{*2})^{1/2}} \quad (3.2.20)$$

To determine the free parameters in the model, these equations must be fit to the observed properties of nuclear matter. The nuclear binding energy is given by

$$\frac{\mathcal{E}}{\rho_B} - M = -16.10 \text{ MeV} \quad (3.2.21)$$

with an equilibrium density given by 1.3 fm^{-3} . With a nucleon mass of 939 MeV and $m_\omega=783 \text{ MeV}$ a fit at the mean field level [48] was found to give values of $g_\sigma^2=109.6$, $g_\omega^2=190.4$ and $m_s=520 \text{ MeV}$.

3.2.1 Relativistic Hartree

The relativistic Hartree contribution, sometimes referred to as the 1-loop vacuum contribution, arises when canceling divergences in the scalar self energy. The correction to the energy is given by

$$\begin{aligned} \Delta\mathcal{E} = & -\frac{\gamma}{16\pi^2} [M^{*4} \ln(M^*/M) + M^3(M - M^*) - \frac{7}{2}M^2(M - M^*)^2 \\ & + \frac{13}{3}M(M - M^*)^3 - \frac{25}{12}(M - M^*)^4] \end{aligned} \quad (3.2.22)$$

Diagrammatically, this contribution comes from the summing of tadpole diagrams as shown by Chin [49]. Including this we still have a self consistent equation of state. This contribution is related to the pressure and energy by

$$P = P_{MF} - \Delta\mathcal{E} \quad (3.2.23)$$

$$\mathcal{E} = \mathcal{E}_{MF} + \Delta\mathcal{E} \quad (3.2.24)$$

If we once again minimize either the pressure or energy we find a modification the effective mass.

$$\begin{aligned} M^* &= M - \frac{g_\sigma^2}{m_\sigma^2} \frac{\gamma}{(2\pi)^3} \int_0^{k_F} d^3k \frac{M^*}{(k^2 + M^{*2})^{1/2}} \\ &+ \frac{g_\sigma^2}{m_\sigma^2} \frac{1}{\pi^2} \left[M^{*3} \ln(M^*/M) - M^2 * (M^* - M) - \frac{5}{2} M (M^* - M)^2 - \frac{11}{6} (M^* - M)^3 \right] \end{aligned} \quad (3.2.25)$$

A fit at the RHA level [48] was found to give values of $g_\sigma^2=54.3$, $g_\omega^2=102.8$ and $m_s=458$ MeV. As compared with the mean field results, in the RHA a reduction of almost 50% was found for both of the values of the coupling constants.

3.2.2 QHD II MFT

For a more complete model of nuclear matter, we extend our theory to include charged mesons. This includes both the π and ρ meson. This extension along with the Walecka model (QHD-I) is generally referred to as QHD-II. To begin with we include the ρ meson triplet. It is coupled to the isospin of the nucleon so that a scalar is formed. The extended Lagrangian is given by

$$\begin{aligned} \mathcal{L} &= \bar{\psi} \left[i\rlap{\not{\partial}} - g_\omega\psi - M + g_\sigma\sigma + g_\rho\boldsymbol{\rho}^a\tau_a - i\frac{g_A}{f_\pi}\gamma_5\rlap{\not{\partial}}\pi_a\frac{\tau_a}{2} \right] \psi \\ &- \frac{1}{2}m_\sigma^2\sigma^2 + \frac{1}{2}m_\omega^2\omega^2 + \frac{1}{2}m_\rho\rho_\mu^a\rho_a^\mu - \frac{1}{2}m_\pi^2\pi_a^2 \end{aligned} \quad (3.2.26)$$

where τ_a refers to the Pauli matrices for isospin. As before, we begin by looking at the theory in the relativistic mean field approximation. The expectation value of the pion in the mean field should vanishes due to parity considerations. The resulting mean field lagrangian is then given by

$$\begin{aligned} \mathcal{L}_{MF} &= \bar{\psi} \left[i\rlap{\not{\partial}} - (M - g_\sigma\bar{\sigma}) + (\mu - g_\omega\bar{\omega}_0 - g_\rho\tau_3\bar{\rho}_{03})\gamma^0 \right] \psi \\ &- \frac{1}{2}m_\sigma^2\bar{\sigma}^2 + \frac{1}{2}m_\omega^2\bar{\omega}_0^2 + \frac{1}{2}m_\rho\bar{\rho}_{03}^2 \end{aligned} \quad (3.2.27)$$

Where τ_3 is the third isospin component which is 1/2 for the proton and -1/2 for the neutron. The energy density and pressure now become

$$\begin{aligned} \mathcal{E}^{(1)} = & \frac{g_\omega}{2m_\omega^2} n_B^2 - \frac{m_\sigma^2}{2g_\sigma} (M - M^*)^2 + \frac{g_\rho^2}{8m_\rho^2} n_{\rho 03} \\ & + \frac{2}{(2\pi)^3} \left[\int_0^{k_{f_p}} d^3 p E^*(p) + \int_0^{k_{f_n}} d^3 p E^*(p) \right] + \Delta \mathcal{E}(M^*) \end{aligned} \quad (3.2.28)$$

$$\begin{aligned} P = & \frac{g_\omega}{2m_\omega^2} n_B^2 + \frac{m_\sigma^2}{2g_\sigma} (M - M^*)^2 + \frac{g_\rho^2}{8m_\rho^2} n_{\rho 03} \\ & + \frac{1}{3} \frac{2}{(2\pi)^3} \left[\int_0^{k_{f_p}} d^3 p p^2 / E^*(p) + \int_0^{k_{f_n}} d^3 p p^2 / E^*(p) \right] - \Delta \mathcal{E}(M^*) \end{aligned} \quad (3.2.29)$$

We now have the addition of the ρ mass contribution as well as the separation of the fermi piece as the according to their isospin. Notice that as $k_{f_n} = k_{f_p}$ we recover our original expression for the energy density. The mean fields and densities are now given as follows.

$$\bar{\rho}_{03} = \frac{1}{2} \frac{g_\rho}{m_\rho^2} n_{\rho 03} \quad (3.2.30)$$

$$\bar{\omega}_0 = \frac{g_\omega}{m_\omega^2} n_B \quad (3.2.31)$$

$$\bar{\sigma} = \frac{g_\sigma^2}{m_\sigma^2} n_s \quad (3.2.32)$$

$$n_{\rho 03} = n_p - n_n \quad (3.2.33)$$

$$n_p = \frac{k_p^3}{3\pi^2} \quad (3.2.34)$$

$$n_n = \frac{k_n^3}{3\pi^2} \quad (3.2.35)$$

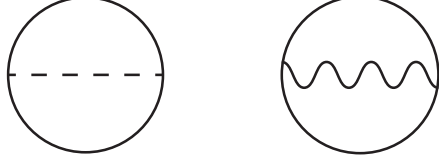


Figure 3.1: Two loop diagrams for scalar and vector

3.3 Two-loop Diagrams

Moving beyond the mean field, we would now like to calculate the two loop contributions to the equation of state. These were first calculated at zero temperature by Furnstal, Perry and Serot [48]. The corresponding diagrams are shown in Fig. 3.1.

We begin by writing the contributions to the total energy density.

$$\mathcal{E}^{(2)}(M^*, \rho_B) = \mathcal{E}^{(1)}(M^*, \rho_B) \quad (3.3.36)$$

$$+ \frac{1}{2} g_\sigma^2 \int \frac{d^4 k}{(2\pi)^4} \int \frac{d^4 q}{(2\pi)^4} \text{tr} [G^*(k) G^*(q)] \Delta^0(k - q) \quad (3.3.37)$$

$$- \frac{1}{2} g_\omega^2 \int \frac{d^4 k}{(2\pi)^4} \int \frac{d^4 q}{(2\pi)^4} \text{tr} [G^*(k) \gamma^\mu G^*(q) \gamma_\mu] D^0(k - q) \quad (3.3.38)$$

Here Δ^0 and D^0 are the scalar and vector propagators respectively. The last two terms correspond to the diagrams in Fig. 3.1.

$$\Delta^0(k) = \frac{1}{k^2 - m_\sigma^2 + i\epsilon} \quad (3.3.39)$$

$$D_{\mu\nu}^0 = \frac{-g_{\mu\nu}}{k^2 - m_\omega^2 + i\epsilon} \quad (3.3.40)$$

The nucleon propagator can be separated into two parts given as the Feynman contribution and the finite density contribution. This can be done by taking the pole structure into account [51] (also appendix). It is given as follows.

$$G^*(p) = (\gamma_\mu p^\mu + M^{*2}) \left[\frac{1}{p^2 - M^{*2} + i\epsilon} + \frac{i\pi}{E^*(p)} \delta(p^0 - E^*(p)) \Theta(k_f - |p|) \right] \quad (3.3.41)$$

$$= G_F^*(p) + G_D^*(p) \quad (3.3.42)$$

Here

$$E^{*2}(p) = p^2 + (M^*)^2 \quad (3.3.43)$$

and

$$M^* = M - g_\sigma \bar{\sigma} \quad (3.3.44)$$

$$k_f^2 = \mu^2 - m^2 \quad (3.3.45)$$

G_F^* refers to the usual fermi propagator and G_D^* is the finite density piece. Using this we see that the 2-loop contributions separate into three parts. The first is referred to as the exchange contribution and represents the exchange of momenta between 2 nucleons. The second is analogous to the Lamb Shift in atomic physics. The third is a vacuum fluctuation. The diagrammatic breakdown is show in Fig. 3.2. The equations are as follows.

$$\mathcal{E}^{(2)}(M^*, \rho_B) = \mathcal{E}^{(1)}(M^*, \rho_B) + \mathcal{E}_{ex}^{(2)}(M^*, \rho_B) + \mathcal{E}_{LS}^{(2)}(M^*, \rho_B) + \mathcal{E}_{VF}^{(2)}(M^*, \rho_B) \quad (3.3.46)$$

Exchange

$$\mathcal{E}_{EX} = \frac{1}{2} g_\sigma^2 \int \frac{d^4 k}{(2\pi)^4} \int \frac{d^4 q}{(2\pi)^4} tr [G_D^*(k) G_D^*(q)] \Delta^0(k - q) \quad (3.3.47)$$

$$- \frac{1}{2} g_\omega^2 \int \frac{d^4 k}{(2\pi)^4} \int \frac{d^4 q}{(2\pi)^4} tr [G_D^*(k) \gamma^\mu G_D^*(q) \gamma_\mu] D^0(k - q) \quad (3.3.48)$$

Lamb Shift

$$\mathcal{E}_{LS}^{(2)} = g_\sigma^2 \int \frac{d^4 k}{(2\pi)^4} \int \frac{d^4 q}{(2\pi)^4} tr [G_D^*(k) G_F^*(q)] \Delta^0(k - q) \quad (3.3.49)$$

$$- g_\omega^2 \int \frac{d^4 k}{(2\pi)^4} \int \frac{d^4 q}{(2\pi)^4} tr [G_D^*(k) \gamma^\mu G_F^*(q) \gamma_\mu] D^0(k - q) \quad (3.3.50)$$

Vacuum

$$\mathcal{E}_{VF}^{(2)} = \frac{1}{2} g_\sigma^2 \int \frac{d^4 k}{(2\pi)^4} \int \frac{d^4 q}{(2\pi)^4} tr [G_F^*(k) G_F^*(q)] \Delta^0(k - q) \quad (3.3.51)$$

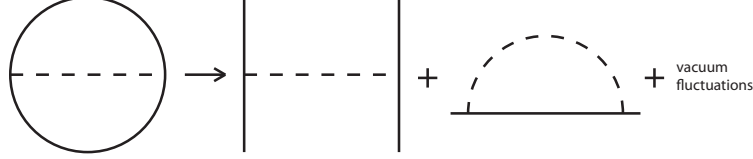


Figure 3.2: 2-loop Contributions

$$-\frac{1}{2}g_\omega^2 \int \frac{d^4k}{(2\pi)^4} \int \frac{d^4q}{(2\pi)^4} \text{tr} [G_F^*(k)\gamma^\mu G_F^*(q)\gamma_\mu] D^0(k-q) \quad (3.3.52)$$

The first of these terms can be analyzed straightforwardly. The other two require renormalization to remove divergences. These contributions were then analyzed numerically. It was found that the size of these were too large to be treated as perturbations and the loop expansion was found not to be convergent. This is illustrated in figure 3.4. As one can see, the separate contributions are all large compared to the RHA contribution. However, one solution, proposed by Prakash Ellis and Kapusta addressed this issue by considering the fact that nucleons are composite particle rather than point particles. To accomplish this they introduced form factors into the vertices of the second order diagrams. The form factor they used is

$$f(k^2) = \frac{1}{1 - k^2/\Lambda^2} \quad (3.3.53)$$

where the cutoff parameter Λ is the size of the nucleon. Inserting these they found that the two-loop corrections are vastly reduced. Near the equilibrium the contributions were reduced 10-15%. This is seen in Fig. 3.5. Overall, they were able to show that the introduction of form factors was able to address the problem of exceedingly large loop contributions. However, it would be more satisfying if we could address this issue within the context of the model. Motivated by our previous work with nonlocal theories, in the next section, we will investigate nonlocally modified nuclear matter models as a way to achieve this.

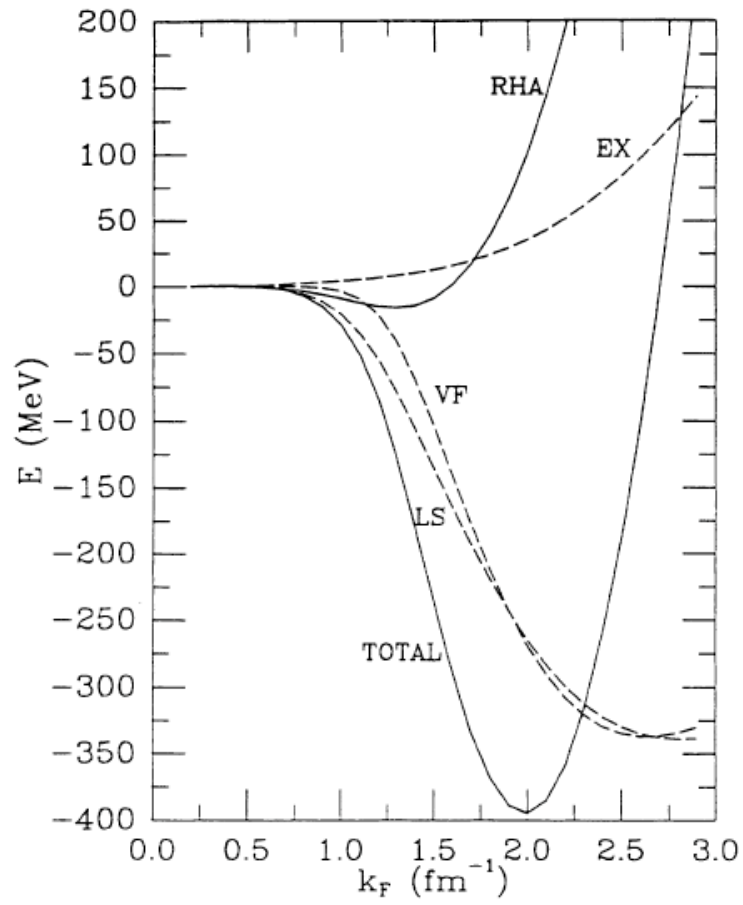


Figure 3.3: Two loop contributions with point vertices. $g_\sigma^2 = 54.3$, $m_\sigma=458$ MeV, $g_\omega^2=102.8$, $m_\omega=783$ MeV [46]

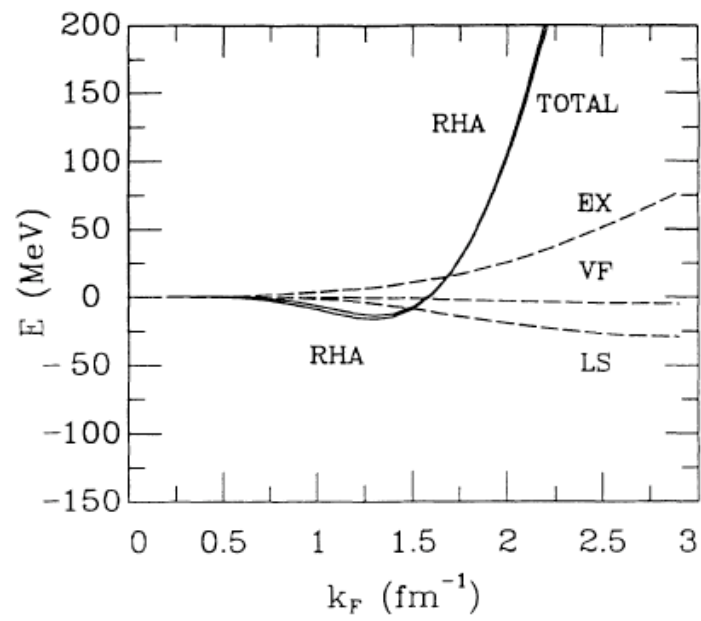


Figure 3.4: Two loop contributions with form factor. [46]

Chapter 4

Nonlocal effective model

4.1 Introduction

As we previously discussed, the traditional study of nuclear matter is done using QHD, and its extension QHD II. At the mean field level it is relatively simple and provides a fit to many properties of nuclear matter. Successful work has been done to improve upon the MFT result as the relativistic Hartree approximation includes 1-loop information. Investigation of the 2-loop contributions have proved troublesome [48]. In their work they found that this contribution yielded enormous results. Solutions to this issue have been proposed [46] which soften these large contributions by the introduction of a form factor at the loop vertices. However, it would be more satisfying to have a model that provided such results rather than insertion of form factors by hand.

One method for doing this is to consider a nonlocal modification to the theory. Nonlocal theories have been studied in many areas of physics, though much of the motivation for this has come from String Field Theory. However, some work has been done in the context of nuclear physics [50], though not involving the two-loop corrections. Motivated by our previous work [4] we introduce the nonlocality in the form of a gaussian. Contrary to before, we include this in the interaction between nucleons and mesons.

In the following section we give our modified Lagrangian and calculate the resulting two-loop contributions. We note that the mean field should not be affected. We then extend our model to include the π and ρ mesons and calculate the two-loop contributions from these. Finally we look at the numerical results and compare to previously published

results.

4.2 Nonlocal Model

We would like to find a model in which the two-loop contributions would be softened. Motivated by our previous work with nonlocal fields, and the idea that we should not treat nucleons as point particles, we introduce a nonlocal interaction into the Walecka model for nuclear matter. While this isn't the only choice [50] (also appendix), we follow the path that leaves the baryon chemical potential unchanged. Our model is given as follows.

$$\mathcal{L}_{NLNM} = \bar{\psi} \left[i\not{\partial} - g_{\omega} e^{-\partial^2/2\Lambda^2} \psi - M + g_{\sigma} e^{-\partial^2/2\Lambda^2} \sigma \right] \psi - \frac{1}{2} m_{\sigma}^2 \sigma^2 + \frac{1}{2} m_{\omega}^2 \omega^2 \quad (4.2.1)$$

In this model we see that the vertex is modified by a momentum dependent factor. We introduce a new parameter Λ which we consider to be on the order of nucleon size. For simplicity, we consider this new parameter to be the same for all interactions. However, we could allow it to be different for each meson which may lead to more interesting behavior.

Interactions of this form lead to a modification of the vertices as follows. The vertex diagrams are given in Fig. 4.1

$$g_{\sigma} \rightarrow g_{\sigma} e^{(\mathbf{p}_1 - \mathbf{p}_2)^2 / 2\Lambda^2} \quad (4.2.2)$$

For the vector vertex we have

$$g_{\omega} \rightarrow g_{\omega} \gamma^{\mu} e^{(\mathbf{p}_1 - \mathbf{p}_2)^2 / 2\Lambda^2} \quad (4.2.3)$$

4.2.1 MFT and Hartree Approximation

To begin with we would like to comment on our modification in the mean field. As shown in the work by Chin[49], the energy up to the Hartree Level can be given diagrammatically by a sum of repeated tadpole diagrams. For example, at lowest order, the contribution is given by diagrams 1a and 1b in Chin. Since there is zero momentum exchange in the tadpole diagrams, we are left with the usual self energies. From this, we see that our vertex would not lead to a modification of the mean field results.



Figure 4.1: Scalar(dotted) and Vector(wavy) interaction vertices

4.2.2 Two-loop diagrams

We would now like to compute the two-loop contributions. The corresponding diagrams are the same as before and are shown in Fig 3.2. As show in Appendix C we can proceed the same way as we did previously. The nucleon propagator can be separated into two parts given as the Feynman contribution an the finite density contribution. This can be done by taking the pole structure into account. It is given once again as follows.

$$G^*(p) = (\gamma_\mu p^\mu + M^{*2}) \left[\frac{1}{p^2 - M^{*2} + i\epsilon} + \frac{i\pi}{E^*(p)} \delta(p^0 - E^*(p)) \Theta(k_f - |p|) \right] \quad (4.2.4)$$

$$= G_F^*(p) + G_D^*(p) \quad (4.2.5)$$

where

$$E^{*2}(p) = p^2 + (M^*)^2 \quad (4.2.6)$$

and

$$M^* = M - g_\sigma \bar{\sigma} \quad (4.2.7)$$

$$k_f^2 = \mu^2 - m^2 \quad (4.2.8)$$

The total energy density at the two loop level is then given by

$$\mathcal{E}^{(2)}(M^*, \rho_B) = \mathcal{E}^{(1)}(M^*, \rho_B) \quad (4.2.9)$$

$$+\frac{1}{2}g_s^2 \int \frac{d^4k}{(2\pi)^4} \int \frac{d^4q}{(2\pi)^4} tr \left[G^*(k)e^{(k-q)^2/2\Lambda^2} G^*(q)e^{(k-q)^2/2\Lambda^2} \right] \Delta^0(k-q) \quad (4.2.10)$$

$$-\frac{1}{2}g_v^2 \int \frac{d^4k}{(2\pi)^4} \int \frac{d^4q}{(2\pi)^4} tr \left[G^*(k)\gamma^\mu e^{(k-q)^2/2\Lambda^2} G^*(q)\gamma_\mu e^{(k-q)^2/2\Lambda^2} \right] D^0(k-q) \quad (4.2.11)$$

$$+\text{counter terms} \quad (4.2.12)$$

where Δ^0 and D^0 are the scalar and vector propagators respectively.

$$\Delta^0(k) = \frac{1}{k^2 - m_\sigma^2 + i\epsilon} \quad (4.2.13)$$

$$D_{\mu\nu}^0 = \frac{-g_{\mu\nu}}{k^2 - m_\omega^2 + i\epsilon} \quad (4.2.14)$$

To calculate the two-loop contribution we insert the nucleon propagator. This decomposes the two-loop energy into 3 pieces, the exchange, Lamb shift and vacuum contributions. The second two need to be renormalized.

$$\mathcal{E}^{(2)}(M^*, \rho_B) = \mathcal{E}^{(1)}(M^*, \rho_B) + \mathcal{E}_{ex}^{(2)}(M^*, \rho_B) + \mathcal{E}_{LS}^{(2)}(M^*, \rho_B) + \mathcal{E}_{VF}^{(2)}(M^*, \rho_B) \quad (4.2.15)$$

Exchange

$$\mathcal{E}_{EX} = \frac{1}{2}g_s^2 \int \frac{d^4k}{(2\pi)^4} \int \frac{d^4q}{(2\pi)^4} tr [G_D^*(k)G_D^*(q)] e^{(k-q)^2/\Lambda^2} \Delta^0(k-q) \quad (4.2.16)$$

$$-\frac{1}{2}g_v^2 \int \frac{d^4k}{(2\pi)^4} \int \frac{d^4q}{(2\pi)^4} tr [G_D^*(k)\gamma^\mu G_D^*(q)\gamma_\mu] e^{(k-q)^2/\Lambda^2} D^0(k-q) \quad (4.2.17)$$

Lamb Shift

$$\mathcal{E}_{LS}^{(2)} = g_s^2 \int \frac{d^4k}{(2\pi)^4} \int \frac{d^4q}{(2\pi)^4} tr \left[G_D^*(k)e^{(k-q)^2/2\Lambda^2} G_F^*(q)e^{(k-q)^2/2\Lambda^2} \right] \Delta^0(k-q) \quad (4.2.18)$$

$$-g_v^2 \int \frac{d^4k}{(2\pi)^4} \int \frac{d^4q}{(2\pi)^4} tr \left[G_D^*(k)\gamma^\mu e^{(k-q)^2/2\Lambda^2} G_F^*(q)\gamma_\mu e^{(k-q)^2/2\Lambda^2} \right] D^0(k-q) \quad (4.2.19)$$

Vacuum

$$\mathcal{E}_{VF}^{(2)} = \frac{1}{2}g_s^2 \int \frac{d^4k}{(2\pi)^4} \int \frac{d^4q}{(2\pi)^4} \text{tr} \left[G_F^*(k) e^{(k-q)^2/2\Lambda^2} G_F^*(q) e^{(k-q)^2/2\Lambda^2} \right] \Delta^0(k-q) \quad (4.2.20)$$

$$-\frac{1}{2}g_v^2 \int \frac{d^4k}{(2\pi)^4} \int \frac{d^4q}{(2\pi)^4} \text{tr} \left[G_F^*(k) \gamma^\mu e^{(k-q)^2/2\Lambda^2} G_F^*(q) \gamma_\mu e^{(k-q)^2/2\Lambda^2} \right] D^0(k-q) \quad (4.2.21)$$

In Hing, McIntire and Serot [47], a paper in 2007 investigated the contributions from the two loop diagrams for the σ , ω and ρ . In their work they considered the Lagrangian to be a truncation of a chirally invariant one [52]. They showed that the vacuum and Lamb shift diagrams can be rewritten in terms of pieces that would have been contained in the Lagrangian before the truncation. From this they argued that the exchange contribution is the the only one that needs to be calculated. In this fashion, they essentially perform a regularization. Following their work, we will explicitly calculate the two loop exchange contributions.

We begin by computing the trace over spinor indices and integrating over the zero component of the momentum. Doing so we find the following expressions for the scalar and vector pieces.

$$\begin{aligned} \mathcal{E}_{ex-\sigma} &= \gamma g_s^2 \int \frac{d^3q}{(2\pi)^3} \frac{d^3k}{(2\pi)^3} \frac{\theta(k_f - k)}{2E^*(k)} \frac{\theta(k_f - q)}{2E^*(q)} \\ &\quad \times \left[\frac{E^*(k)E^*(q) + M^{*2} - \mathbf{k} \cdot \mathbf{q}}{(\mathbf{k} - \mathbf{q})^2 - [E^*(k) - E^*(q)]^2 + m_s^2} \right] e^{[(E^*(k) - E^*(q))^2 - (\mathbf{k} - \mathbf{q})^2/\Lambda^2]} \quad (4.2.22) \end{aligned}$$

$$\begin{aligned} \mathcal{E}_{ex-\omega} &= \gamma 2g_v^2 \int \frac{d^3q}{(2\pi)^3} \frac{d^3k}{(2\pi)^3} \frac{\theta(k_f - k)}{2E^*(k)} \frac{\theta(k_f - q)}{2E^*(q)} \\ &\quad \times \left[\frac{E^*(k)E^*(q) - 2M^{*2} - \mathbf{k} \cdot \mathbf{q}}{(\mathbf{k} - \mathbf{q})^2 - [E^*(k) - E^*(q)]^2 + m_v^2} \right] e^{[(E^*(k) - E^*(q))^2 - (\mathbf{k} - \mathbf{q})^2/\Lambda^2]} \quad (4.2.23) \end{aligned}$$

To push forward analytically we can do the following.

$$\begin{aligned} &\left[\frac{E^*(k)E^*(q) + M^{*2} - \mathbf{k} \cdot \mathbf{q}}{(\mathbf{k} - \mathbf{q})^2 - [E^*(k) - E^*(q)]^2 + m_s^2} \right] \\ &= \frac{1}{2} \left[1 + \frac{4M^{*2} - m_s^2}{2E^*(k)E^*(q) - 2M^{*2} + m_s^2 - 2\mathbf{k} \cdot \mathbf{q}} \right] \quad (4.2.24) \end{aligned}$$

$$\begin{aligned}
& \left[\frac{E^*(k)E^*(q) - 2M^{*2} - \mathbf{k} \cdot \mathbf{q}}{(\mathbf{k} - \mathbf{q})^2 - [E^*(k) - E^*(q)]^2 + m_s^2} \right] \\
&= \frac{1}{2} \left[1 - \frac{2M^{*2} + m_v^2}{2E^*(k)E^*(q) - 2M^{*2} + m_v^2 - 2\mathbf{k} \cdot \mathbf{q}} \right] \quad (4.2.25)
\end{aligned}$$

Doing the angular integrations we find

$$\begin{aligned}
\mathcal{E}_{ex-\sigma} &= \gamma g_s^2 \frac{\Lambda^2}{26\pi^4} \int_0^{k_f} dq \int_0^{k_f} dk \frac{kq}{\sqrt{(k^2 + M^{*2})(q^2 + M^{*2})}} \\
&\quad \times \sinh\left(\frac{2kq}{\Lambda^2}\right) e^{\left[\frac{2M^{*2}}{\Lambda^2} - \frac{2\sqrt{(k^2 + M^{*2})(q^2 + M^{*2})}}{\Lambda^2}\right]} \\
&- \frac{\gamma g_s^2}{27\pi^4} \int_0^{k_f} dq \int_0^{k_f} dk \frac{kq(4M^{*2} - m_s^2)e^{m_s^2/\Lambda^2}}{\sqrt{(k^2 + M^{*2})(q^2 + M^{*2})}} \\
&\quad \times \left[Ei\left(-\frac{(A_s - 2kq)}{\Lambda^2}\right) - Ei\left(-\frac{(A_s + 2kq)}{\Lambda^2}\right) \right] \quad (4.2.26)
\end{aligned}$$

$$\begin{aligned}
\mathcal{E}_{ex-\omega} &= \gamma 2g_v \frac{\Lambda^2}{26\pi^4} \int_0^{k_f} dq \int_0^{k_f} dk \frac{kq}{\sqrt{(k^2 + M^{*2})(q^2 + M^{*2})}} \\
&\quad \times \sinh\left(\frac{2kq}{\Lambda^2}\right) e^{\left[\frac{2M^{*2}}{\Lambda^2} - \frac{2\sqrt{(k^2 + M^{*2})(q^2 + M^{*2})}}{\Lambda^2}\right]} \\
&+ \frac{2\gamma g_v^2}{27\pi^4} \int_0^{k_f} dq \int_0^{k_f} dk \frac{kq(2M^{*2} + m_v^2)e^{m_v^2/\Lambda^2}}{\sqrt{(k^2 + M^{*2})(q^2 + M^{*2})}} \\
&\quad \times \left[Ei\left(-\frac{(A_v - 2kq)}{\Lambda^2}\right) - Ei\left(-\frac{(A_v + 2kq)}{\Lambda^2}\right) \right] \quad (4.2.27)
\end{aligned}$$

Where

$$Ei(x) = - \int_{-x}^{\infty} \frac{e^{-t}}{t} dt \quad (4.2.28)$$

$$A_i = 2E^*(k)E^*(q) - 2M^{*2} + m_i^2 \quad (4.2.29)$$

4.2.3 QHD-II

Nonlocal ρ

We would like to calculate the additional two-loop diagram for the ρ . To do this we extend our nonlocal model to include a nonlocal interaction with the ρ

$$\mathcal{L} = \bar{\psi} \left[i\rlap{\not{\partial}} - g_\omega e^{-\partial^2/2\Lambda^2} \phi - M + g_\sigma e^{-\partial^2/2\Lambda^2} \sigma + \frac{1}{2} g_\rho e^{\frac{-\partial^2}{2\Lambda^2}} \rlap{\not{\phi}}^a \tau_a \right] \psi - \frac{1}{2} m_\sigma^2 \sigma^2 + \frac{1}{2} m_\omega^2 \omega^2 + \frac{1}{2} m_\rho \rho_\mu^a \rho_a^\mu \quad (4.2.30)$$

where the ρ propagator is given by

$$R_{\mu\nu,ab}^0(k) = \frac{-g_{\mu\nu} \delta_{ab}}{k^2 - m_\rho^2 + i\epsilon} \quad (4.2.31)$$

and τ_a are the Pauli matrices.

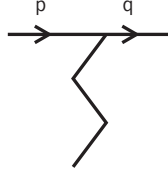


Figure 4.2: ρ interaction vertex

The two loop rho exchange contribution is given by

$$\mathcal{E}_{EX} = -\frac{1}{2} \int \frac{d^4 k}{(2\pi)^4} \int \frac{d^4 q}{(2\pi)^4} \text{tr} \left[(g_\rho \frac{\tau_a}{2} \gamma^\mu) G_D^*(k) (g_\rho \frac{\tau_b}{2} \gamma^\nu) G_D^*(q) \right] e^{(k-q)^2/\Lambda^2} R_{\mu\nu,ab}^0(k-q) \quad (4.2.32)$$

For this case we have equal fermi momenta and find an expression similar to the vector contribution.



Figure 4.3: Two loop diagrams for the rho

$$\mathcal{E}_{ex-\rho} = 6g_\rho^2 \int \frac{d^3\mathbf{q}}{(2\pi)^3} \frac{d^3\mathbf{k}}{(2\pi)^3} \frac{\theta(k_f - \mathbf{k})}{2E^*(\mathbf{k})} \frac{\theta(k_f - \mathbf{q})}{2E^*(\mathbf{q})} \times \left[\frac{E^*(k)E^*(q) - 2M^{*2} - \mathbf{k} \cdot \mathbf{q}}{(\mathbf{k} - \mathbf{q})^2 - [E^*(k) - E^*(q)]^2 + m_\rho^2} \right] e^{[(E^*(k) - E^*(q))^2 - (\mathbf{k} - \mathbf{q})^2 / \Lambda^2]} \quad (4.2.33)$$

$$\begin{aligned} \mathcal{E}_{ex-\rho} &= 6g_\rho^2 \frac{\Lambda^2}{2^6 \pi^4} \int_0^{k_f} dq \int_0^{k_f} dk \frac{kq}{\sqrt{(k^2 + M^{*2})(q^2 + M^{*2})}} \\ &\quad \times \sinh\left(\frac{2kq}{\Lambda^2}\right) e^{\left[\frac{2M^{*2}}{\Lambda^2} - \frac{2\sqrt{(k^2 + M^{*2})(q^2 + M^{*2})}}{\Lambda^2}\right]} \\ &+ \frac{6g_\rho^2}{2^7 \pi^4} \int_0^{k_f} dq \int_0^{k_f} dk \frac{kq(2M^{*2} + m_\rho^2)e^{m_\rho^2/\Lambda^2}}{\sqrt{(k^2 + M^{*2})(q^2 + M^{*2})}} \\ &\quad \times \left[Ei\left(-\frac{(A_\rho - 2kq)}{\Lambda^2}\right) - Ei\left(-\frac{(A_\rho + 2kq)}{\Lambda^2}\right) \right] \quad (4.2.34) \end{aligned}$$

where definitions are given in 4.2.30 and 4.2.31. The coupling constant g_ρ is determined by the value of the symmetry coefficient at nuclear equilibrium. This is given as follows.

$$\left(\frac{g_\rho}{m_\rho}\right)^2 \frac{k_F^3}{12\pi^2} + \frac{k_F^2}{6(k_F^2 + M^{*2})^{1/2}} = 32.5\text{MeV} \quad (4.2.35)$$

Nonlocal π

We now include the π meson with the derivative coupling. We modify this interaction as before with our gaussian term. The Lagrangian for this is as follows.

$$\mathcal{L} = \bar{\psi} \left[i\rlap{\not{\partial}} - g_\omega e^{-\partial^2/2\Lambda^2} \psi - M + g_\sigma e^{-\partial^2/2\Lambda^2} \sigma + g_\rho e^{-\partial^2/2\Lambda^2} \rho^a \frac{\tau_a}{2} - i \frac{g_A}{f_\pi} \gamma_5 \rlap{\not{\partial}} \pi_a \frac{\tau_a}{2} e^{-\partial^2/2\Lambda^2} \right] \psi$$

$$- \frac{1}{2} m_\sigma^2 \sigma^2 + \frac{1}{2} m_\omega^2 \omega^2 + \frac{1}{2} m_\rho \rho_\mu^a \rho_a^\mu - \frac{1}{2} m_\pi^2 \pi_a^2 \quad (4.2.36)$$

$$\mathcal{E}_{ex-\pi} = \frac{g_A}{2f_\pi^2} \int \frac{d^4 k}{(2\pi)^4} \frac{d^4 q}{(2\pi)^4} \Delta_\pi^{ab}(k-q) \text{tr} \left[(\rlap{\not{k}} - \rlap{\not{q}}) \gamma_5 \frac{\tau_a}{2} G^*(k) e^{(k-q)^2/2\Lambda} (\rlap{\not{k}} - \rlap{\not{q}}) \gamma_5 \frac{\tau_b}{2} e^{(k-q)^2/2\Lambda} G^*(q) \right]$$

$$(4.2.37)$$

$$\mathcal{E}_{ex-\pi} = \gamma M^{*2} \frac{g_A}{f_\pi^2} \left(\frac{5\gamma - 8}{16} \right) \int \frac{d^2 k}{(2\pi)^2} \frac{d^3 q}{(2\pi)^3} \frac{\theta(k_f - \mathbf{k})}{2E^*(\mathbf{k})} \frac{\theta(k_f - \mathbf{q})}{2E^*(\mathbf{q})}$$

$$\times \left[\frac{E^*(k)E^*(q) - M^{*2} - \mathbf{k} \cdot \mathbf{q}}{(\mathbf{k} - \mathbf{q})^2 - [E^*(k) - E^*(q)]^2 + m_\pi^2} \right] e^{[(E^*(k) - E^*(q))^2 - (\mathbf{k} - \mathbf{q})^2/\Lambda^2]} \quad (4.2.38)$$

$$\left[\frac{E^*(k)E^*(q) - M^{*2} - \mathbf{k} \cdot \mathbf{q}}{(\mathbf{k} - \mathbf{q})^2 - [E^*(k) - E^*(q)]^2 + m_\pi^2} \right]$$

$$= \frac{1}{2} \left[1 - \frac{m_\pi^2}{2E^*(k)E^*(q) - 2M^{*2} + m_\pi^2 - 2\mathbf{k} \cdot \mathbf{q}} \right] \quad (4.2.39)$$

$$\mathcal{E}_{ex-\pi} = \frac{\gamma g_A^2}{f_\pi^2} \left(\frac{5\gamma - 8}{16} \right) \frac{M^{*2} \Lambda^2}{2^6 \pi^4} \int_0^{k_f} dq \int_0^{k_f} dk \frac{kq}{\sqrt{(k^2 + M^{*2})(q^2 + M^{*2})}}$$

$$\times \sinh \left(\frac{2kq}{\Lambda^2} \right) e^{\left[\frac{2M^{*2}}{\Lambda^2} - \frac{2\sqrt{(k^2 + M^{*2})(q^2 + M^{*2})}}{\Lambda^2} \right]}$$

$$+ \frac{\gamma g_A^2}{f_\pi^2} \left(\frac{5\gamma - 8}{16} \right) \frac{M^{*2}}{2^7 \pi^4} \int_0^{k_f} dq \int_0^{k_f} dk \frac{kq(-m_\pi^2) e^{m_\pi^2/\Lambda^2}}{\sqrt{(k^2 + M^{*2})(q^2 + M^{*2})}}$$

$$\times \left[Ei \left(-\frac{(A_\pi - 2kq)}{\Lambda^2} \right) - Ei \left(-\frac{(A_\pi + 2kq)}{\Lambda^2} \right) \right] \quad (4.2.40)$$

4.3 Numerical Work

In this section we will look at the case of symmetric nuclear matter which will allow us to give a comparison to similar calculations found in the literature. We begin by treating

the loop contributions as perturbations. We compare the two loop scalar and vector contributions using a parameter set fit at the RHA level. The parameter set used for this is FPS in table 4.1. We will show that parameters can be readjusted to fit nuclear equilibrium requirements. We then look at the comparison of the pion contribution in our non local theory as compared to usual coupling [47]. We then minimize the full two loop energy to calculate the effective mass. We find that this has almost no effect on the two loop energy.

We start by analyzing the scalar and vector exchange contributions. We compare with the results of Furnstahl et al [48] as well as those of Prakash et al [46]. In Fig 4.4 we see the suppression of the modified 2 loop contribution as compared to the usual contribution for the same parameter set. At the equilibrium energy we find a suppression of about 8% in our model compared to 10-15% [46] when using the cut off in eqn 3.53 . In our model we find a softer behavior when using a parameter of the same size. Adding this contribution to the the one-loop contribution we see that the energy is only slightly modified. This is shown in Fig. 4.5 The equilibrium value is shifted to a slightly smaller equilibrium density. In Fig 4.6 the coupling constants are refitted to nuclear equilibrium. The new values of couplings become $g_\sigma^2=54.4$ and $g_\omega^2=92.7$. We see that qualitatively this makes little difference in the shape of the nuclear binding curve.

In Fig. 4.7 the two loop exchange contribution for the pion is show in comparison with the unmodified contribution[47]. Here the suppression is even more slight than in the previous case. Combining this with the previous result we plot the total energy in Fig 4.8. Once again the curve is refitted to nuclear equilibrium. The results for the coupling are give as set Fit 1 in table 4.1. We that while the scalar coupling is only slightly modified, the vector coupling is reduced by about 12%

The effective mass was then calculated by minimizing the full two loop energy. The result of this show in Fig. 4.9 in comparison with the RHA result. The effective mass is only slightly changed for values above nuclear equilibrium. The two loop energy calculated with the two loop effective mass was found to be almost the same when compared to using the RHA effective mass.

Finally we calculate the contribution form the two-loop rho exchange. This is given in Fig. 4.10. For this case, no comparison is shown as none was found in the literature. Qualitatively the ρ contribution has a some what different shape than the previous

contributions, although quantitatively it is of a similar magnitude. In Fig. 4.11 we plot its addition to the total energy. We see that it brings the closer to nuclear equilibrium. A readjustment of the scalar and vector couplings in this case only require a slight change. We find values of $g_\sigma^2=54.0$ and $g_\omega^2=98.8$.

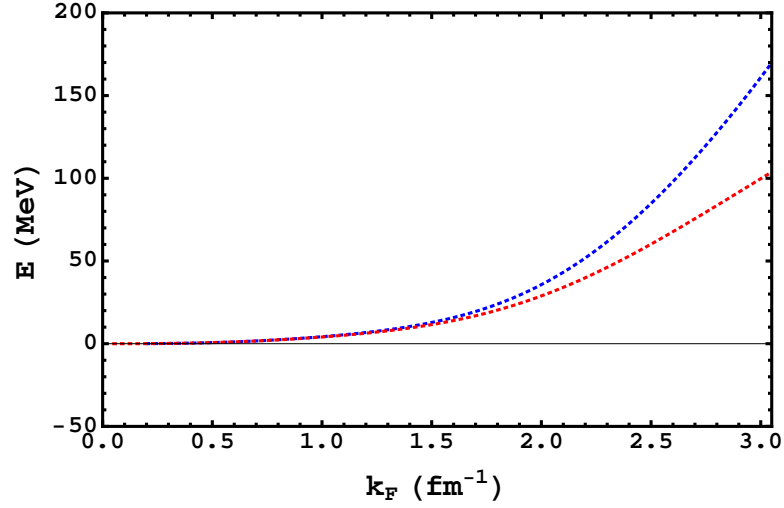


Figure 4.4: Comparison of the usual two-loop σ and ω contribution (blue) with the nonlocal one (red). At the equilibrium value of 1.3 fm^{-1} we find a reduction of about 8%

Table 4.1: Parameter Sets				
	g_σ^2	g_ω^2	$m_\sigma(\text{MeV})$	$m_\omega(\text{MeV})$
FPS	54.3	102.8	458	783
Fit 1	55.8	90.8	458	783
HMS	99.5	148.0	506.5	783

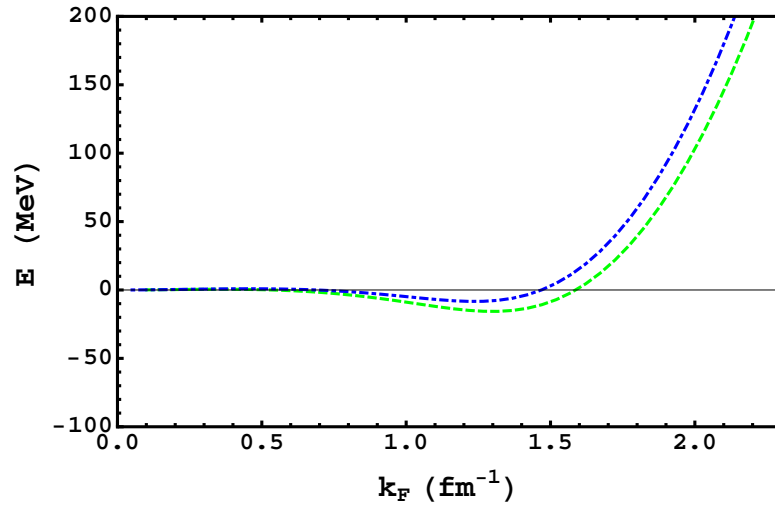


Figure 4.5: Comparison of the one-loop energy (green) with the total two-loop energy with the σ and ω (blue,dotdashed)

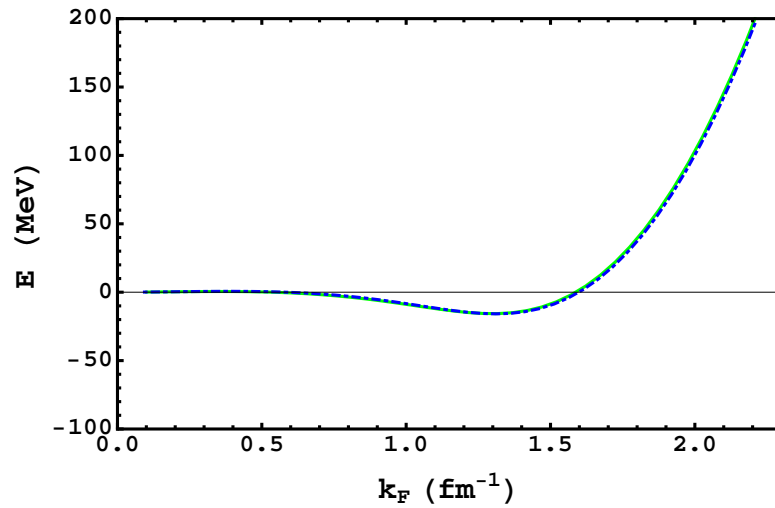


Figure 4.6: Adjustment of couplings to fit total energy to nuclear equilibrium. One-loop (green). Total two-loop energy with the σ and ω (blue, dotdashed)

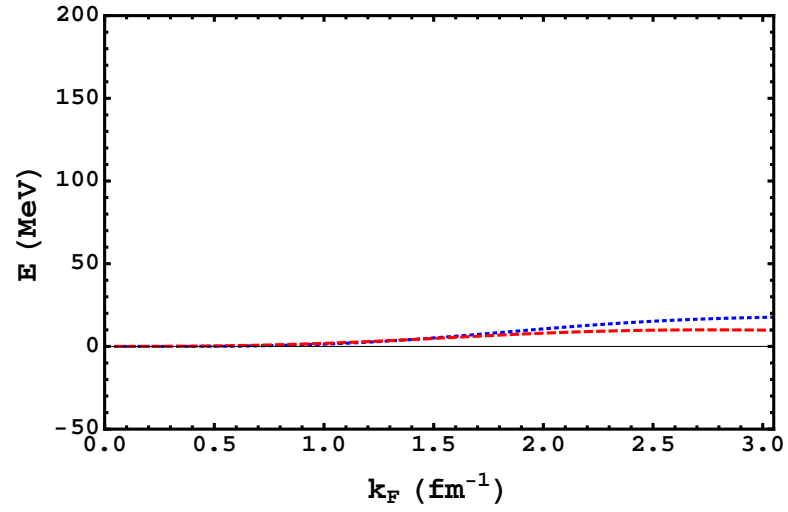


Figure 4.7: Two-loop exchange contribution comparison for the π . Conventional (blue-dotted). Nonlocal (red-dashed).

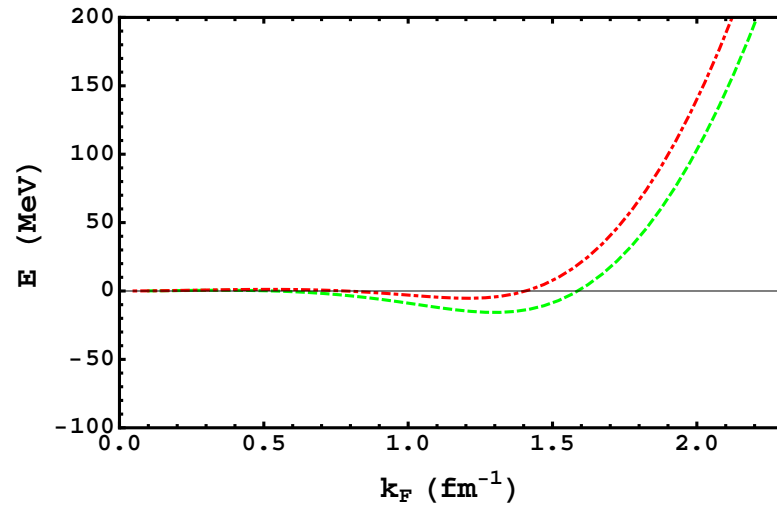


Figure 4.8: Total energy including the the σ, ω, π . Two-loop contributions (red-dotted) compared with RHA (green-dashed)

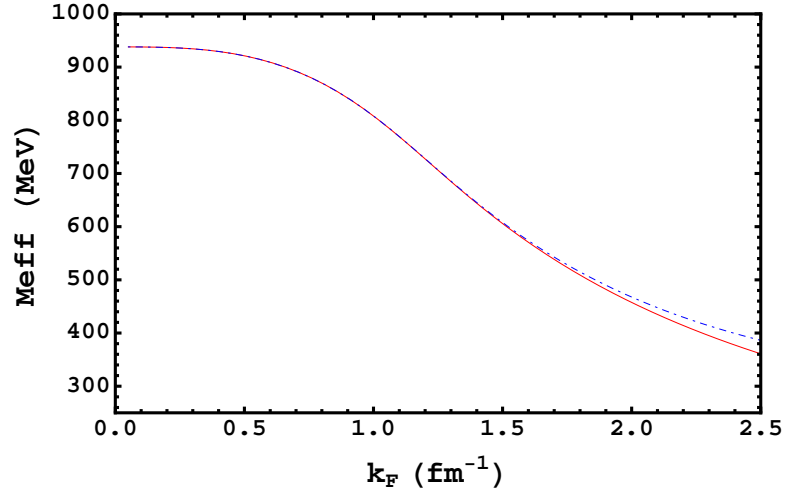


Figure 4.9: Effective Mass determined at the one loop level(red,solid) and two-loop level(blue,dotdashed)

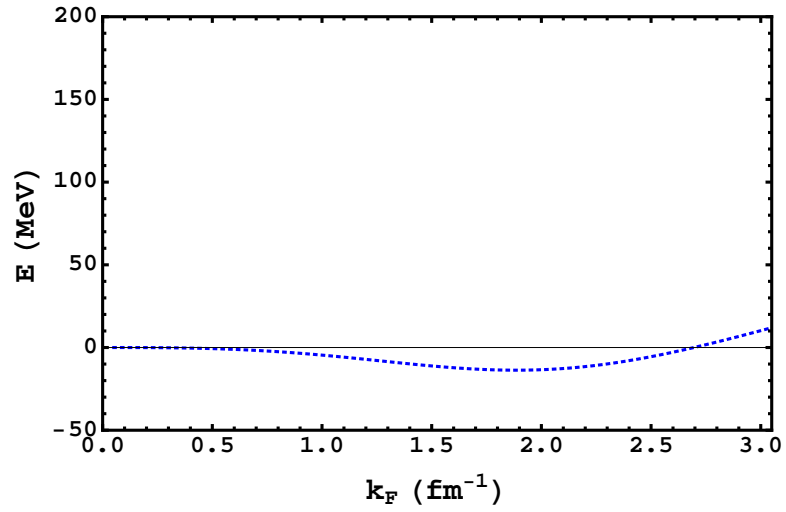


Figure 4.10: Two-loop exchange contribution for the nonlocal ρ meson

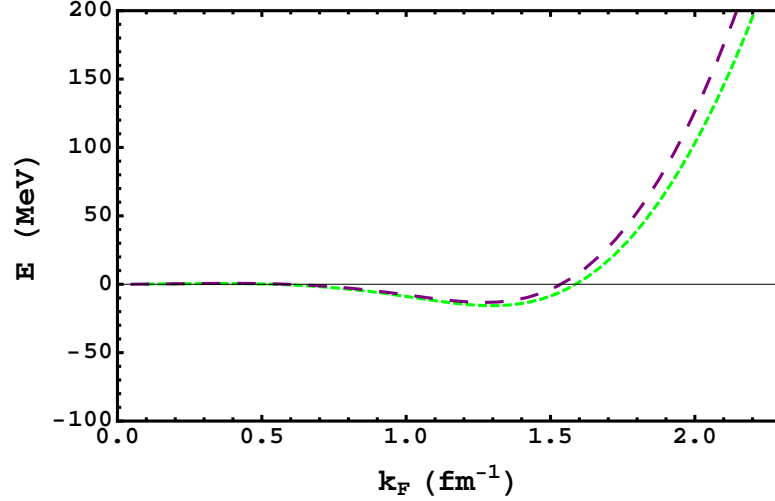


Figure 4.11: Comparison of one-loop energy (green-dashed) with the total two-loop including the $\sigma, \omega, \pi, \rho$ (purple-large dashed)

4.4 Conclusion

We investigated a theory for nuclear matter motivated by the finite size of nucleons and mesons. In spirit, our model is similar to the form factor introduced by in [46] as well the the work done in [50]. However, we consider an interaction within in the Lagrangian rather than ad-hoc vertex correction. We see that in the mean field, this new interaction leaves the mean field result unchanged and only appears when the loop diagrams are considered. We compute the two loop exchange contributions within this theory and compare to previous results found in the literature. We found that the suppression is weaker that what was found for the harder cutoff [46]. Additionally we extended the model to include the pion and rho meson. We extremized the energy at the two loop level and refit the parameters to reproduce nuclear equilibrium. We found that the effective mass at the two loop level is relatively unchanged when compared to the one RHA level. The contribution from the ρ meson was then investigated.

While our results don't reveal a drastic departure from previous work, we were able to incorporate our interaction into the Lagrangian. An additional possibility would be to consider would be to have different parameters for each meson rather than a single

one. This way the two loop contributions could be suppressed individually. This may be of use when considering applications such as neutron stars.

Chapter 5

Conclusion and Discussion

In this thesis we have discussed nonlocal fields and presented investigations of a nonlocal scalar field at finite temperature as well as the use of nonlocal interactions in an effective field theory for nuclear matter.

In Chapter 1 we discussed some of the history of nonlocal fields and how they have been used in physics.

In Chapter 2, motivated by previous work on similar actions and by the possibility of cosmological applications we investigated the nonlocal action describing the tachyon in SFT. We found that the presence of the nonlocality does not change the results as drastically as one might think.

In Chapter 3 we reviewed the work done on effective field theories in nuclear matter and discussed issues that arise when moving beyond the mean field. This led us into Chapter 4 where we discussed an a modification to the usual effective field theory motivated by previous work on nonlocal fields.

In both cases we found similar qualitative results. In the areas where there were differences or improvements these effects were found to be slight. In both case, however, explorations in terms of different parameters, could possibly lead to more interesting results. In the case of the tachyon this would involve investigating the limit where m/M is large. In the nuclear matter case we could consider the effects of introducing different Λ parameters for different interactions. Another possibility would be the application to neutron stars.

References

- [1] H. Yukawa, "Quantum Field Theory of Nonlocal Fields. Part I: Free Fields," *Phys. Rev.* **77**, 219 (1950).
H. Yukawa, "Quantum Field Theory of Nonlocal Fields. Part II: Irreducible Fields and Their Interactions," *Phys. Rev.* **80**, 1047 (1950).
- [2] S. Deser and R. P. Woodard, "Nonlocal Cosmology," *Phys.Rev.Lett.* **99**:111301,2007
- [3] D. Even, J. W. Moffat, G. Kleppe and R. P. Woodard, "Nonlocal Regularizations of Gauge Theories," *Phys. Rev. D* **43** 499, 1991
- [4] Tirthabir Biswas, Joseph I. Kapusta, Abrahm Reddy, "Thermodynamics of String Field Theory Motivated Nonlocal Models," *JHEP* **12** (2012) 008 [arXiv:1201.1580]
- [5] A. Sen, "Tachyon Dynamics in Open String Theory," *Int. J. Mod. Phys.* **A20**, 5513-5656 (2005).
- [6] A. Sen, "Rolling Tachyon," *JHEP* **0204**, 048 (2002).
A. Sen, "Tachyon matter," *JHEP* **0207**, 065 (2002).
- [7] E. Witten, "Noncommutative Geometry and String Field Theory," *Nucl. Phys.* **B268**, 253 (1986).
- [8] V. A. Kostelecky and S. Samuel, "The Static Tachyon Potential in the Open Bosonic String Theory," *Phys. Lett.* **B207**, 169 (1988).

- V. A. Kostelecky and S. Samuel, "On a Nonperturbative Vacuum for the Open Bosonic String," Nucl. Phys. **B336**, 263 (1990).
- [9] I. Y. Aref'eva, A. S. Koshelev, D. M. Belov and P. B. Medvedev, "Tachyon Condensation in Cubic Superstring Field Theory," Nucl. Phys. **B638**, 3 (2002).
- [10] G. Calcagni and G. Nardelli, "Tachyon Solutions in Boundary and Cubic String Field Theory," Phys. Rev. D **78**, 126010 (2008).
- [11] W. Taylor and B. Zwiebach, "D-branes, Tachyons, and String Field Theory," in *Strings, Branes and Extra Dimensions* (TASI 2001), World Scientific, ed. S. S. Gubser and J. D. Lykken. arXiv:hep-th/0311017.
- [12] G. Calcagni and G. Nardelli, "Kinks in open superstring field theory", Nucl. Phys. **B823**, 234 (2009). [arXiv:0904.3744].
- [13] B. Dragovich, "Zeta Strings," arXiv:hep-th/0703008.
B. Dragovich, "Zeta Nonlocal Scalar Fields," Theor. Math. Phys. **157**, 1671 (2008).
- [14] N. Moeller and B. Zwiebach, "Dynamics with Infinitely Many Time Derivatives and Rolling Tachyons," JHEP **0210**, 034 (2002).
- [15] I. Y. Aref'eva and L.V. Joukovskaya, "Time Lumps in Nonlocal Stringy Models and Cosmological Applications," JHEP **0510**, 087 (2005).
I. Y. Aref'eva, A. S. Koshelev and S. Y. Vernov, "Crossing of the $w=-1$ Barrier by D3-brane Dark Energy Model," Phys. Rev. D **72**, 064017 (2005).
I. Y. Aref'eva, "Nonlocal String Tachyon as a Model for Dark Energy," arXiv:astro-ph/0410443v2.
- [16] N. Barnaby, T. Biswas and J. M. Cline, "p-adic Inflation," JHEP **0704**, 056 (2007). [arXiv:hep-th/0612230].
J. E. Lidsey, "Stretching the Inflaton Potential with Kinetic Energy," Phys. Rev. D **76**, 043511(2007).
N. J. Nunes and D. J. Mulryne, "Non-linear Nonlocal Cosmology," AIP Conf. Proc. **1115**, 329 (2009).

- N. Barnaby and J. M. Cline, "Large Nongaussianity from Nonlocal Inflation," *JCA* **0707**, 017 (2007).
- N. Barnaby and J. M. Cline, "Predictions from Nongaussianity from Nonlocal Inflation," *JCA* **0806**, 030 (2007).
- [17] I. Y. Aref'eva and L. V. Joukovskaya and S. Y. Vernov, "Bouncing and Accelerating Solution in Nonlocal String Models," *JHEP* **0707**, 087 (2007).
- [18] L. Joukovskaya, "Dynamics in Nonlocal Cosmological Models Derived from String Field Theory," *Phys. Rev. D* **76**, 105007 (2007).
- A. Koshelev, "Nonlocal SFT Tachyon and Cosmology," *JHEP* **0704**, 029 (2007).
- [19] G. Calcagni, M. Montobbio and G. Nardelli, "Route to Nonlocal Cosmology" *Phys. Rev. D* **76**, 126001 (2007).
- [20] G. Calcagni and G. Nardelli, "Cosmological Rolling Solutions of Nonlocal Theories," *Int. J. Mod. Phys. D* **19**, 230 (2010).
- [21] I. Y. Aref'eva, L. V. Joukovskaya, and S. Y. Vernov, "Dynamics in Nonlocal Linear Models in the Friedmann-Robertson-Walker Metric," *J. Phys. A: Math. Theor.* **41**, 304003 (2008).
- [22] J. W. Moffat, "Ultraviolet Complete Electroweak Model Without a Higgs Particle," *Eur. Phys. J. Plus* **126**, 53 (2011).
- J. W. Moffat and V. T. Toth, "Redesigning Electroweak Theory: Does the Higgs Particle Exist?," arXiv:0908.0780 [hep-ph].
- J. W. Moffat and V. T. Toth, "A Finite Electroweak Model without a Higgs Particle," arXiv:0812.1991 [hep-ph].
- J. W. Moffat, "Electroweak Model Without A Higgs Particle," arXiv:0709.4269 [hep-ph].
- [23] S. Deser and R. P. Woodard, "Nonlocal Cosmology," *Phys. Rev. Lett.* **99**, 111301 (2007).
- [24] Tomi Koivisto, "Dynamics of Nonlocal Cosmology," *Phys. Rev. D* **77**, 123513 (2008).

- [25] T. Biswas, E. Gerwick, T. Koivisto and A. Mazumdar, "Towards Singularity and Ghost Free Theories of Gravity,"
T. Biswas, A. Mazumdar and W. Siegel, "Bouncing universes in string-inspired gravity," *JCAP* **0603**, 009 (2006).
- [26] J. Khoury, "Fading Gravity and Self-inflation," *Phys. Rev. D* **76**, 123513 (2007).
- [27] E. Elizalde, E. O. Pozdeeva and S. Y. Vernov, "De Sitter Universe in Non-local Gravity," arXiv:1110.5806 [astro-ph.CO].
- [28] J. W. Moffat, "Ultraviolet Complete Quantum Gravity," *Eur. Phys. J. Plus* **126**, 43 (2011).
- [29] L. Modesto, "Super-renormalizable Quantum Gravity," arXiv:1107.2403 [hep-th].
- [30] S. Capozziello, E. Elizalde, S. 'i. Nojiri and S. D. Odintsov, "Accelerating cosmologies from non-local higher-derivative gravity," *Phys. Lett.* **B671**, 193 (2009). [arXiv:0809.1535 [hep-th]].
- [31] P. G. O. Freund and M. Olson, "Nonarchimedean Strings," *Phys. Lett.* **B199**, 186 (1987).
P. G. O. Freund and E. Witten, "Adelic String Amplitudes," *Phys. Lett.* **B199**, 191 (1987).
L. Brekke, P. G. O. Freund, M. Olson and E. Witten, "Nonarchimedean String Dynamics," *Nucl. Phys.* **B302**, 365 (1998).
- [32] T. Biswas, J. A. R. Cembranos and J. I. Kapusta "Thermodynamics and Cosmological Constant of nonlocal Field Theories from p-Adic Strings", *JHEP* **10**, 048 (2010).
T. Biswas, J. A. R. Cembranos and J. I. Kapusta "Thermal Duality and Hagedorn Transition from p-adic Strings," *Phys. Rev. Lett.* **104**, 021601 (2010).
- [33] J. J. Atick and E. Witten, "The Hagedorn Transition and the Number of Degrees of Freedom of String Theory," *Nucl. Phys.* **B310**, 291 (1988).

- [34] J. A. Minahan, "Mode interactions of the tachyon condensate in p-adic string theory," JHEP **0103**, 028 (2001).
- [35] T. Biswas, M. Grisaru and W. Siegel, "Linear Regge Trajectories from Worldsheet Lattice Parton Field Theory," Nucl. Phys. **B708**, 317 (2005).
- [36] Robert Bluhm, "Particle Fields at Finite Temperature from String Field Theory," Phys. Rev. D **43**, 4042 (1991).
- [37] A. Nayeri, R. H. Brandenberger and C. Vafa, "Producing a Scale-invariant Spectrum of Perturbations in a Hagedorn Phase of String Cosmology," Phys. Rev. Lett. **97**, 021302 (2006).
- R. H. Brandenberger, S. Kanno, J. Soda, D. A. Easson, J. Khoury, P. Martineau, A. Nayeri and S. P. Patil, "More on the Spectrum of Perturbations in String Gas Cosmology," JCAP **0611**, 009 (2006).
- T. Biswas, R. Brandenberger, A. Mazumdar and W. Siegel, "Non-perturbative Gravity, Hagedorn Bounce and CMB," JCAP **0712**, 011 (2007).
- J. Magueijo and L. Pogosian, "Could Thermal Fluctuations Seed Cosmic Structure?," Phys. Rev. D **67**, 043518 (2003).
- J. Magueijo and P. Singh, "Thermal Fluctuations in Loop Cosmology," Phys. Rev. D **76**, 023510 (2007).
- Y.-F. Cai, W. Xue, R. Brandenberger and X.-M. Zhang, "Thermal Fluctuations and Bouncing Cosmologies," JCAP **0906**, 037 (2009).
- J. Magueijo, L. Smolin and C. R. Contaldi, "Holography and the Scale-invariance of Density Fluctuations," Class. Quant. Grav. **24**, 3691 (2007).
- J.-P. Wu and Y. Ling, "Thermal Non-Gaussianity in Near-Milne Universe," Phys. Lett. **B684**, 177-180 (2010).
- J. Magueijo, "Near-Milne Realization of Scale-invariant Fluctuations," Phys. Rev. D **76**, 123502 (2007).
- [38] A. Berera, "Warm inflation," Phys. Rev. Lett. **75**, 3218 (1995).

- [39] Y. Volovich, “Numerical Study of Nonlinear Equations with Infinite Number of Derivatives,” *J. Phys. A* **36**, 8685 (2003).
- V. S. Vladimirov and Y. I. Volovich, “On the Nonlinear Dynamical Equation in the p-adic String Theory,” *Theor. Math. Phys.* **138**, 297 (2004) [*Teor. Mat. Fiz.* **138**, 355 (2004)].
- V. S. Vladimirov, “On the Equation of the p-adic Open String for the Scalar Tachyon Field,” *Izv. Math.* **69**, 487 (2005).
- D. V. Prokhorenko, “On Some Bonlinear Integral Equation in the (Super)String Theory,” arXiv:math-ph/0611068.
- N. Barnaby and N. Kamran, “Dynamics with Infinitely Many Derivatives: Variable Coefficient Equations,” *JHEP* **0812**, 022 (2008).
- N. Barnaby and N. Kamran, “Dynamics with Infinitely Many Derivatives: The Initial Value Problem,” *JHEP* **0802**, 008 (2008).
- G. Calcagni, M. Montobbio and G. Nardelli, “Localization of Nonlocal Theories,” *Phys. Lett.* **B662**, 285 (2008).
- P. Gorka, H. Prado and E. G. Reyes, ”Functional Calculus via Laplace Transform and Equations with Infinitely Many Derivatives,” *J. Math. Phys.* **51**, 103512 (2010).
- [40] J. I. Kapusta and C. Gale, *Finite Temperature Field Theory*, Cambridge University Press, Cambridge, 2nd edition, 2006.
- [41] T. D. Lee and M. Margulies, *Phys. Rev. D* **11**, 1591 (1975).
- [42] P. Arnold and O. Espinosa, *Phys. Rev. D* **47**, 3546 (1993); Erratum **50**, 6662 (1994).
- [43] J. D. Walecka, ”A Theory of Highly Condensed Matter,” *Ann. Phys.* **83**, 491 (1974)
- [44] N. K. Glendenning, *Compact Stars*, Springer-Verlag, New York, 2nd edition, 1997.
- [45] B. D. Serot and J. D. Walecka, *Advances in Nuclear Physics: Vol 16*, Plenum Press, New York, 1st edition, 1986.
- [46] Madappa Prakash Paul J. Ellis and Joseph I. Kapusta, ”Relativistic Matter with Composite Nucleons,” *Phys. Rev. C* **45**, 2518 (1992).

- [47] Ying Hu, Jeff McIntire and B. D. Serot, "Two Loop Corrections for Nuclear Matter in a Covariant Effective Field Theory," *Nuc. Phys. A* **794**, 187 (2007).
- [48] R. J. Furnstahl, R. J. Perry and B. D. Serot, "Two Loop Corrections for Nuclear Matter in the Walecka Model," *Phys. Rev. C* **40**, 321 (1989).
- [49] S. A. Chin, "A Relativistic Many-Body Theory of High Density Matter," *Ann. Phys.* **108**, 301 (1977).
- [50] V. K. Mishra, G. Fai and P. C. Tandy, "Nonlocal Field Theory for Nuclear Matter," *Phys. Rev. C* **46**, 1143 (1992).
- [51] Barry Freedman and Larry McLerran, "Fermions and gauge vector mesons at finite temperature and density. I. Formal techniques," *Phys. Rev. D* **16**, 1130 (1977).
- [52] R. J. Furnstahl, B. D. Serot and H. Tang *Nucl. Phys.* **A615** (1997) 441; *Nucl. Phys.* **A640** (1998) 505(E).

Appendix A

Theta Functions

The Theta-function are complex valued functions define as follows

$$\theta_1(\nu, \tau) = 2 \sum_{n=0}^{\infty} (-1)^n e^{i\pi\tau(n+1/2)^2} \sin[\pi(2n+1)\nu] \quad (\text{A.0.1})$$

$$\theta_2(\nu, \tau) = 2 \sum_{n=0}^{\infty} e^{i\pi\tau(n+1/2)^2} \cos[\pi(2n+1)\nu] \quad (\text{A.0.2})$$

$$\theta_3(\nu, \tau) = 1 + 2 \sum_{n=1}^{\infty} e^{i\pi\tau n^2} \cos[2\pi n\nu] \quad (\text{A.0.3})$$

$$\theta_0(\nu, \tau) = 1 + 2 \sum_{n=1}^{\infty} (-1)^n e^{i\pi\tau n^2} \cos[2\pi n\nu] \quad (\text{A.0.4})$$

They have the following relations

$$\theta_1\left(\frac{\nu}{\tau}, \frac{-1}{\tau}\right) = \frac{1}{i} \sqrt{\frac{\tau}{i}} e^{i\pi\nu^2/\tau} \theta_1(\nu, \tau) \quad (\text{A.0.5})$$

$$\theta_2\left(\frac{\nu}{\tau}, \frac{-1}{\tau}\right) = \sqrt{\frac{\tau}{i}} e^{i\pi\nu^2/\tau} \theta_0(\nu, \tau) \quad (\text{A.0.6})$$

$$\theta_3\left(\frac{\nu}{\tau}, \frac{-1}{\tau}\right) = \sqrt{\frac{\tau}{i}} e^{i\pi\nu^2/\tau} \theta_3(\nu, \tau) \quad (\text{A.0.7})$$

$$\theta_0\left(\frac{\nu}{\tau}, \frac{-1}{\tau}\right) = \sqrt{\frac{\tau}{i}} e^{i\pi\nu^2/\tau} \theta_2(\nu, \tau) \quad (\text{A.0.8})$$

For our purposes we are interested in θ_3 . We start with the definition.

$$\theta_3(0, \tau) = 1 + 2 \sum_{n=1}^{\infty} e^{i\pi\tau n^2} = \sum_{n=-\infty}^{\infty} e^{i\pi\tau n^2} \quad (\text{A.0.9})$$

Let us set $i\pi\tau = -s^2$ putting this in the other relationship we find.

$$\theta_3\left(0, \frac{i\pi}{s^2}\right) = \frac{s}{\sqrt{\pi}} \theta_3\left(0, \frac{-s^2}{i\pi}\right) \quad (\text{A.0.10})$$

Combining the last 2 equations and multiplying both sides by $\sqrt{\pi}/s$ we find the relationship used in the text

$$\frac{\sqrt{\pi}}{s} \sum_{n=-\infty}^{\infty} e^{-\pi^2 n^2 / s^2} = \sum_{n=-\infty}^{\infty} e^{-n^2 s^2} \quad (\text{A.0.11})$$

Appendix B

Nonlocal Fermion

B.1 Nonlocal Fermion

One model we can consider is one put forth by Mishra, Fai and Tandy. In this model is the nonlocality if included as

$$\mathcal{L}_{NLNM} = \bar{\psi} \left[(i\hat{\not{\partial}} - g_\omega \psi) \hat{F}_\omega - M + g_\sigma \sigma \hat{F}_\sigma \right] \psi - \frac{1}{2} m_\sigma^2 \sigma^2 + \frac{1}{2} m_\omega^2 \omega^2 \quad (\text{B.1.1})$$

where

$$\hat{F}_i = \exp \left[-\beta_i^2 \left(1 - \frac{\partial^2}{M^2} \right) \right] = e^{-\beta_i^2} \sum_{n=0}^{\infty} \left(\frac{\beta_i^2}{M^2} \partial^2 \right)^n \quad (\text{B.1.2})$$

In their paper they investigated this theory in the relativistic Hartree approximation and did not consider loop diagrams. However, it was found that they did not correctly include the baryon chemical potential. Here we determine how to correctly include the chemical potential by finding the conserved current for this theory associated with its U(1) symmetry. To do this, we consider the Lagrangian for a nonlocal fermion given by

$$\mathcal{L} = \bar{\psi} \left[i\hat{\not{\partial}} \hat{F} - M \right] \psi \quad (\text{B.1.3})$$

where we have set the F's equal. We will later need the equations of motion to find the conserved current for this theory. Varying with respect to $\bar{\psi}$ we find

$$\left[i\gamma^\mu \partial_\mu \hat{F} - M \right] \psi = 0 \quad (\text{B.1.4})$$

Integrating the Lagrangian by parts and dropping surface terms, we can move all derivatives to $\bar{\psi}$. Varying with respect to ψ we find

$$\left[-i\partial_\mu \hat{F}\bar{\psi}\gamma^\mu - M\bar{\psi}\right] = 0 \quad (\text{B.1.5})$$

B.1.1 Conserved Current

We now would like to find the conserved current for this theory. Under a U(1) symmetry $\psi \rightarrow \psi e^{-i\alpha}$ and $\bar{\psi} \rightarrow \bar{\psi} e^{i\alpha}$. We allow α to depend on x . We transform the Lagrangian according to these rules and apply the equation of motion for α . The lagrangian transforms as

$$\mathcal{L} \rightarrow \mathcal{L}(\partial\alpha, \partial^2\alpha, \dots) \quad (\text{B.1.6})$$

For higher derivative theories the equation of motion is given by

$$\frac{\partial\mathcal{L}}{\partial\alpha} - \partial_\mu \frac{\partial\mathcal{L}}{\partial(\partial_\mu\alpha)} + \partial_{\mu\nu} \frac{\partial\mathcal{L}}{\partial(\partial_{\mu\nu}\alpha)} - \partial_{\mu\nu\gamma} \frac{\partial\mathcal{L}}{\partial(\partial_{\mu\nu\gamma}\alpha)} + \dots = 0 \quad (\text{B.1.7})$$

Since the transformed Lagrangian is only a function of the derivatives of alpha, we have

$$\partial_\mu \left[\frac{\partial\mathcal{L}}{\partial(\partial_\mu\alpha)} - \partial_\nu \frac{\partial\mathcal{L}}{\partial(\partial_{\mu\nu}\alpha)} + \partial_{\nu\gamma} \frac{\partial\mathcal{L}}{\partial(\partial_{\mu\nu\gamma}\alpha)} - \dots \right] = 0 \quad (\text{B.1.8})$$

The quantity inside the bracket gives a conserved current. Calculating this order by order we find (here we have suppressed a factor of $e^{-\beta^2}$)

$$\begin{aligned} j^\sigma &= \bar{\psi}\gamma^\sigma\psi + \left(\frac{\beta^2}{M^2}\right) [\bar{\psi}\gamma^\mu\partial_\mu\partial^\sigma\psi - \partial^\sigma\bar{\psi}\gamma^\mu\partial_\mu\psi + \partial^2\bar{\psi}\gamma^\sigma\psi] \\ &+ \frac{1}{2!} \left(\frac{\beta^2}{M^2}\right)^2 [\bar{\psi}\gamma^\mu\partial_\mu\partial^\sigma\partial^2\psi - \partial^\sigma\bar{\psi}\gamma^\mu\partial_\mu\partial^2\psi + \partial^2\bar{\psi}\gamma^\sigma\partial^2\psi - \partial_\mu\partial^2\bar{\psi}\gamma^\mu\partial^\sigma\psi + \partial_\mu\partial^\sigma\partial^2\bar{\psi}\gamma^\mu\psi] \\ &+ \frac{1}{3!} \left(\frac{\beta^2}{M^2}\right)^3 [\bar{\psi}\gamma^\mu\partial_\mu\partial^\sigma\partial^4\psi - \partial^\sigma\bar{\psi}\gamma^\mu\partial_\mu\partial^4\psi + \partial^2\bar{\psi}\gamma^\sigma\partial^4\psi - \partial_\mu\partial^2\bar{\psi}\gamma^\mu\partial^\sigma\partial^2\psi + \partial_\mu\partial^2\bar{\psi}\gamma^\sigma\partial^\mu\partial^2\psi \\ &\quad - \partial^\sigma\partial^2\bar{\psi}\gamma^\mu\partial_\mu\partial^2\psi + \partial^4\bar{\psi}\gamma^\sigma\partial^2\psi - \partial_\mu\partial^4\bar{\psi}\gamma^\mu\partial^\sigma\psi + \partial_\mu\partial^\sigma\partial^4\bar{\psi}\gamma^\mu\psi] + \dots \end{aligned} \quad (\text{B.1.9})$$

Checking that this is conserved we find

$$\partial_\sigma j^\sigma = \bar{\psi}\gamma^\sigma\partial_\sigma\psi + \partial_\sigma\bar{\psi}\gamma^\sigma + \left(\frac{\beta^2}{M^2}\right) [\bar{\psi}\gamma^\sigma\partial_\sigma\partial^2\psi + \partial_\sigma\partial^2\bar{\psi}\gamma^\sigma\psi]$$

$$\begin{aligned}
& + \frac{1}{2!} \left(\frac{\beta^2}{M^2} \right)^2 [\bar{\psi} \gamma^\sigma \partial_\sigma \partial^4 \psi + \partial_\sigma \partial^4 \bar{\psi} \gamma^\sigma \psi] + \frac{1}{3!} \left(\frac{\beta^2}{M^2} \right)^3 [\bar{\psi} \gamma^\sigma \partial_\sigma \partial^6 \psi + \partial_\sigma \partial^6 \bar{\psi} \gamma^\sigma \psi] + \dots \\
& = \bar{\psi} \gamma^\sigma \partial_\sigma F \psi + \partial_\sigma F \bar{\psi} \gamma^\sigma \psi = -iM \bar{\psi} \psi + iM \bar{\psi} \psi = 0 \tag{B.1.10}
\end{aligned}$$

after using the equations of motion for ψ and $\bar{\psi}$.

To use the current, we need to put it in a more tractable form. To do this, we once again integrate by part while dropping the surface terms. This gives

$$\begin{aligned}
j^\mu & = \bar{\psi} \gamma^\mu \psi + \left(\frac{\beta^2}{M^2} \right) [2\bar{\psi} \not{\partial} \partial^\mu \psi + \bar{\psi} \gamma^\mu \partial^2 \psi] + \frac{1}{2!} \left(\frac{\beta^2}{M^2} \right)^2 [4\bar{\psi} \not{\partial} \partial^\mu \partial^2 \psi + \bar{\psi} \gamma^\mu \partial^4 \psi] \\
& \quad + \frac{1}{3!} \left(\frac{\beta^2}{M^2} \right)^3 [6\bar{\psi} \not{\partial} \partial^\mu \partial^4 \psi + \bar{\psi} \gamma^\mu \partial^6 \psi] + \dots \\
& = \bar{\psi} \gamma^\mu \left[1 + \left(\frac{\beta^2}{M^2} \right) \partial^2 + \frac{1}{2!} \left(\frac{\beta^2}{M^2} \right)^2 \partial^4 + \frac{1}{3!} \left(\frac{\beta^2}{M^2} \right)^3 \partial^6 + \dots \right] \psi \\
& + 2 \left(\frac{\beta^2}{M^2} \right) \bar{\psi} \not{\partial} \partial^\mu \left[1 + \left(\frac{\beta^2}{M^2} \right) \partial^2 + \frac{1}{2!} \left(\frac{\beta^2}{M^2} \right)^2 \partial^4 + \frac{1}{3!} \left(\frac{\beta^2}{M^2} \right)^3 \partial^6 + \dots \right] \psi \tag{B.1.11}
\end{aligned}$$

So we have

$$j^\mu = \bar{\psi} \gamma^\mu F \psi + 2 \frac{\beta^2}{M^2} \bar{\psi} \not{\partial} \partial^\mu F \psi \tag{B.1.12}$$

For $\beta = 0$ we see that we recover the conserved current for the local fermion as we would expect.

Alternate Derivation

Here we try a naive approach where we do not expand the exponential.

$$\mathcal{L} = \bar{\psi} [(i\not{\partial})F - M] \psi \tag{B.1.13}$$

Under the transformation $\psi \rightarrow \psi e^{-i\alpha(x)}$ the Lagrangian becomes

$$\mathcal{L} = \bar{\psi} [(i\not{\partial} + \not{\partial}\alpha)F' - M] \psi \tag{B.1.14}$$

$$F' = \exp \left[-\beta^2 \left(1 - \frac{1}{M^2} (\partial^2 - (\partial_\mu \alpha)(\partial^\mu \alpha) - i\partial^\mu \alpha \partial_\mu - i\partial_\mu \alpha \partial^\mu - i\partial^2 \alpha) \right) \right] \tag{B.1.15}$$

$$= F \times F^*(\partial\alpha) \quad (\text{B.1.16})$$

Using

$$F^* = 1 + (F^* - 1) \quad (\text{B.1.17})$$

$$\mathcal{L}' = \mathcal{L} + \bar{\psi}(\not{\partial}\alpha F)\psi + \bar{\psi}[(i\not{\partial} + \not{\partial}\alpha)(F^* - 1)F]\psi \quad (\text{B.1.18})$$

Applying the Euler-Lagrange equation for α we find the current to be

$$\partial_\mu [\bar{\psi}(\gamma^\mu F^* F)\psi + \bar{\psi}(i\not{\partial} + \not{\partial}\alpha)F^{**}F\psi] = 0 \quad (\text{B.1.19})$$

where

$$F^{**} = \frac{\partial F^*}{\partial(\partial_\mu\alpha)} = \frac{-\beta^2}{M^2} [2\partial^\mu\alpha + 2i\partial^\mu] F^* \quad (\text{B.1.20})$$

$$\partial_\mu \left[\bar{\psi}(\gamma^\mu F F^*)\psi + \bar{\psi} F F^* (i\not{\partial} + \not{\partial}\alpha) \frac{-\beta^2}{M^2} [2\partial^\mu\alpha + 2i\partial^\mu] \psi \right] = 0 \quad (\text{B.1.21})$$

Setting α to be a constant we are left with

$$\partial_\mu \left[\bar{\psi}\gamma^\mu F\psi + 2\frac{\beta^2}{M^2}\bar{\psi}\not{\partial}\partial^\mu F\psi \right] = 0 \quad (\text{B.1.22})$$

which is the same as we previously derived.

B.1.2 The partition function

The partition function is given by

$$Z = \text{Tr}^\dagger e^{-\beta(H - \mu\hat{Q})} \quad (\text{B.1.23})$$

The functional integral becomes

$$Z = \int [id\bar{\psi}][d\psi] \exp \left[\int d\tau \int d^3x \mathcal{L} + \mu Q \right] \quad (\text{B.1.24})$$

where \mathcal{L} is the finite temperature form of the Lagrangian and

$$Q = \int d^3x j^0 = \int d^3x \left[\bar{\psi}\gamma^0 e^{-\beta_N^2 \left(1 - \frac{\partial^2}{M^2}\right)} \psi + 2\frac{\beta_N^2}{M^2} \bar{\psi}\not{\partial}\partial^0 e^{-\beta_N^2 \left(1 - \frac{\partial^2}{M^2}\right)} \psi \right] \quad (\text{B.1.25})$$

The partition function becomes

$$Z = \int [id\psi^\dagger][d\psi] \exp \left[\int d\tau \int d^3x \bar{\psi} \left(\left(-\gamma^0 \frac{\partial}{\partial \tau} + i\vec{\gamma} \cdot \nabla \right) e^{-\beta_N^2 \left(1 - \frac{\partial^2}{M^2} \right)} - M \right) \right] \quad (\text{B.1.26})$$

$$+ \mu \left(\gamma^0 e^{-\beta_N^2 \left(1 - \frac{\partial^2}{M^2} \right)} + 2 \frac{\beta_N^2}{M^2} \left(i\gamma^0 \frac{\partial}{\partial \tau} + \vec{\gamma} \cdot \vec{\nabla} \right) \left(i \frac{\partial}{\partial \tau} \right) e^{-\beta_N^2 \left(1 - \frac{\partial^2}{M^2} \right)} \right) \psi \quad (\text{B.1.27})$$

We can now Fourier expand ψ

$$\psi_\alpha(x, \tau) = \frac{1}{\sqrt{V}} \sum_n \sum_p e^{i(px + \omega_n \tau)} \psi_{\alpha;n}(p) \quad (\text{B.1.28})$$

Inserting this into the action we get

$$Z = \left[\prod_n \prod_p \prod_\alpha id\psi_{\alpha;n}^\dagger d\psi_{\alpha;n} \right] e^S \quad (\text{B.1.29})$$

where

$$\sum_n \sum_p \psi_{\alpha;n}^\dagger(p) D_{\alpha\rho} \psi_{\rho;n}(p) \quad (\text{B.1.30})$$

and $D_{\alpha\rho}$ is a matrix given by

$$D = -i\beta \left[\left(-i\omega_n - \gamma^0 \vec{\gamma} \cdot \vec{\nabla} + \mu \right) e^{-\beta_N^2 \left(1 + \frac{p^2 + \omega_n^2}{M^2} \right)} - m\gamma^0 \right. \\ \left. + 2i\mu \left(\frac{\beta_N^2}{M^2} \right) \left(-i\omega_n - \gamma^0 \vec{\gamma} \cdot \vec{p} + \mu \right) (\omega_n) e^{-\beta_N^2 \left(1 + \frac{p^2 + \omega_n^2}{M^2} \right)} \right] \quad (\text{B.1.31})$$

$$D = -i\beta \left\{ \left[-i\omega_n \left(1 + 2i\mu \left(\frac{\beta_N^2}{M^2} \right) \omega_n \right) - \gamma^0 \vec{\gamma} \cdot \vec{p} \left(1 + 2i\mu \left(\frac{\beta_N^2}{M^2} \right) \omega_n \right) + \mu \right] \right. \\ \left. \times e^{-\beta_N^2 \left(1 + \frac{p^2 + \omega_n^2}{M^2} \right)} - m\gamma^0 \right\} \quad (\text{B.1.32})$$

where

$$Z = \det D \quad (\text{B.1.33})$$

Using

$$\ln(\det D) = \text{tr}(\ln D) \quad (\text{B.1.34})$$

we find that

$$\ln Z = \sum_n \sum_p \ln \beta^2 \left\{ \left[\left(\omega_n \left(1 + 2i\mu \left(\frac{\beta_N^2}{M^2} \right) \omega_n \right) + i\mu \right)^2 + p^2 \left(1 + 2i\mu \left(\frac{\beta_N^2}{M^2} \right) \omega_n \right)^2 \right] \times e^{-2\beta_N^2 \left(1 + \frac{p^2 + \omega_n^2}{M^2} \right) + m^2} \right\} \quad (\text{B.1.35})$$

Once again, setting $\beta_N = 0$ we recover the local partition function. Here we have shown that the inclusion of the chemical potential in a theory of the type given by Mishra, Fai and Tandy is in fact much more complicated than they suggested.

Appendix C

Propagator Pole Structure

In this section we examine the splitting of the propagator as given by Furnshal, Perry and Serot in [48]. We start by writing down the two loop contribution in our model for the vector and scalar at finite temperature and density. We then take the zero temperature limit and examine the pole structure. We find that splitting of the propagator into the finite density and Fermi propagator contributions is still valid in our model.

C.1 Finite Temperature

Vector contribution

$$-\frac{1}{2}g_v^2 \int \frac{d^3p}{(2\pi)^3} \frac{d^3q}{(2\pi)^3} \frac{d^3k}{(2\pi)^3} (2\pi)^3 \delta(\mathbf{p} - \mathbf{q} - \mathbf{k}) e^{-\mathbf{k}^2/\Lambda^2} \quad (\text{C.1.1})$$

$$\times T^3 \sum_{n_p, n_q, n_k} \beta \delta_{n_p, n_q + n_k} \frac{\text{Tr} [\gamma^\mu (\not{p} + M) \gamma_\mu (\not{q} + M)] e^{k_0^2/\Lambda^2}}{(k^2 - m_v^2)(p^2 - M^2)(q^2 - M^2)} \quad (\text{C.1.2})$$

Scalar contribution

$$\frac{1}{2}g_s^2 \int \frac{d^3p}{(2\pi)^3} \frac{d^3q}{(2\pi)^3} \frac{d^3k}{(2\pi)^3} (2\pi)^3 \delta(\mathbf{p} - \mathbf{q} - \mathbf{k}) e^{-\mathbf{k}^2/\Lambda^2} \quad (\text{C.1.3})$$

$$\times T^3 \sum_{n_p, n_q, n_k} \beta \delta_{n_p, n_q + n_k} \frac{\text{Tr} [(\not{p} + M)(\not{q} + M)] e^{k_0^2/\Lambda^2}}{(k^2 - m_v^2)(p^2 - M^2)(q^2 - M^2)} \quad (\text{C.1.4})$$

$$p_0 = (2n_p + 1)\pi T i \quad (\text{C.1.5})$$

$$q_0 = (2n_q + 1)\pi T i \quad (\text{C.1.6})$$

$$k_0 = 2n_k \pi T i \quad (\text{C.1.7})$$

From the vector contribution

$$-8T^3 \sum_{n_p, n_q, n_k} \beta \delta_{n_p, n_q + n_k} \frac{(2M - pq) e^{k_0^2/\Lambda^2}}{(k^2 - m_v^2)(p^2 - M^2)(q^2 - M^2)} \quad (\text{C.1.8})$$

We can rewrite the delta function as

$$\beta \delta_{n_p, n_q + n_k} = \int_0^\beta d\theta \exp[\theta(p_0 - q_0 - k_0)] = \frac{\exp[\beta(p_0 - q_0 - k_0)]}{p_0 - q_0 - k_0} \quad (\text{C.1.9})$$

$$-8T \sum_{n_k} \frac{1}{k^2 - m_v^2} T \sum_{n_p} \frac{1}{p^2 - M^2} T \sum_{n_q} \frac{1}{q^2 - M^2} I(k_0, p_0, q_0) \quad (\text{C.1.10})$$

$$I(k_0, p_0, q_0) = \frac{2M - pq}{p_0 - q_0 - k_0} [\exp[\beta(k_0 + q_0)] - \exp[\beta p_0]] e^{k_0^2/2\Lambda} \quad (\text{C.1.11})$$

We would like to evaluate the boson portion by contour integration using

$$T \sum_n f(k_0 = i\omega_n) = \frac{1}{2\pi i} \int_{-i\infty}^{i\infty} dk_0 \frac{1}{2} [f(k_0) + f(-k_0)] \quad (\text{C.1.12})$$

$$+ \frac{1}{2\pi i} \int_{-i\infty+\epsilon}^{i\infty+\epsilon} dk_0 [f(k_0) + f(-k_0)] \frac{1}{e^{\beta k_0} - 1} \quad (\text{C.1.13})$$

along with the residue theorem.

C.2 Zero Temperature Limit

$$\frac{\ln Z_2}{\beta V} = -\frac{1}{2} g_v^2 \int \frac{d^3 p}{(2\pi)^3} \frac{d^3 q}{(2\pi)^3} \frac{d^3 k}{(2\pi)^3} (2\pi)^3 \delta(\mathbf{p} - \mathbf{q} - \mathbf{k}) e^{-\mathbf{k}^2/\Lambda^2} \quad (\text{C.2.14})$$

$$\times T^3 \sum_{n_p, n_q, n_k} \beta \delta_{n_p, n_q + n_k} \frac{\text{Tr} [\gamma^\mu (\not{p} + M) \gamma_\mu (\not{q} + M)] e^{k_0^2/\Lambda^2}}{(k^2 - m_v^2)(p^2 - M^2)(q^2 - M^2)} \quad (\text{C.2.15})$$

$$+ \frac{1}{2} g_s^2 \int \frac{d^3 p}{(2\pi)^3} \frac{d^3 q}{(2\pi)^3} \frac{d^3 k}{(2\pi)^3} (2\pi)^3 \delta(\mathbf{p} - \mathbf{q} - \mathbf{k}) e^{-\mathbf{k}^2/\Lambda^2} \quad (\text{C.2.16})$$

$$\times T^3 \sum_{n_p, n_q, n_k} \beta \delta_{n_p, n_q + n_k} \frac{\text{Tr} [(\not{p} + M)(\not{q} + M)] e^{k_0^2/\Lambda^2}}{(k^2 - m_v^2)(p^2 - M^2)(q^2 - M^2)} \quad (\text{C.2.17})$$

$$p_0 = (2n_p + 1)\pi T i + \mu = ip_4 + \mu \rightarrow n_p = \frac{p_4}{2\pi T} - \frac{1}{2} \rightarrow \Delta n_p = \frac{\Delta p_4}{2\pi T} \quad (\text{C.2.18})$$

$$q_0 = (2n_q + 1)\pi T i + \mu = iq_4 + \mu \rightarrow n_q = \frac{q_4}{2\pi T} - \frac{1}{2} \rightarrow \Delta n_q = \frac{\Delta q_4}{2\pi T} \quad (\text{C.2.19})$$

$$k_0 = 2n_k \pi T i = ik_4 \rightarrow n_k = \frac{k_4}{2\pi T} \rightarrow \Delta n_k = \frac{\Delta k_4}{2\pi T} \quad (\text{C.2.20})$$

$$T \sum_n \rightarrow \int \frac{dk}{2\pi} \quad (\text{C.2.21})$$

$$\beta \delta_{n_p, n_q + n_k} \rightarrow \beta \delta \left(\frac{p_4}{2\pi T} - \frac{1}{2} - \left(\frac{q_4}{2\pi T} - \frac{1}{2} \right) - \frac{k_4}{2\pi T} \right) \quad (\text{C.2.22})$$

$$= 2\pi T \beta \delta(p_4 - q_4 - k_4) \quad (\text{C.2.23})$$

First, consider the vector portion only, as both pieces are similar. At finite density we have

$$-\frac{1}{2} g_v^2 \int \frac{d^3 p}{(2\pi)^3} \frac{d^3 q}{(2\pi)^3} \frac{d^3 k}{(2\pi)^3} (2\pi)^3 \delta(\mathbf{p} - \mathbf{q} - \mathbf{k}) e^{-\mathbf{k}^2/\Lambda^2} \quad (\text{C.2.24})$$

$$\times \int_{-\infty}^{\infty} \frac{dk_4}{2\pi} \frac{dp_4}{2\pi} \frac{dq_4}{2\pi} \frac{-8 [2M^2 + \mathbf{p}\mathbf{q} + (p_4 - i\mu)(q_4 - i\mu)] e^{-k_4^2/\Lambda^2}}{(k_4^2 + E_k^2)((p_4 - i\mu)^2 + E_p^2)((q_4 - i\mu)^2 + E_q^2)} (2\pi) \delta(p_4 - k_4 - q_4) \quad (\text{C.2.25})$$

Let's do the integral over k .

$$-\frac{1}{2} g_v^2 \int \frac{d^3 q}{(2\pi)^3} \frac{d^3 k}{(2\pi)^3} \int_{-\infty}^{\infty} \frac{dp_4}{2\pi} \frac{dq_4}{2\pi} \times \frac{-8 [2M^2 + \mathbf{p}\mathbf{q} + (p_4 - i\mu)(q_4 - i\mu)] e^{-((p_4 - i\mu) - (q_4 - i\mu))^2 - \mathbf{k}^2/\Lambda^2}}{(((p_4 - i\mu) - (q_4 - i\mu))^2 + E_{(p-q)}^2)((q_4 - i\mu)^2 + E_q^2)((p_4 - i\mu)^2 + E_p^2)} \quad (\text{C.2.26})$$

$$= -\frac{1}{2} (-8) g_v^2 \int \frac{d^3 q}{(2\pi)^3} \frac{d^3 k}{(2\pi)^3} \times I \quad (\text{C.2.27})$$

Now we make the shift

$$p'_4 = p_4 - i\mu \quad (\text{C.2.28})$$

and

$$q'_4 = q_4 - i\mu \quad (\text{C.2.29})$$

This pushes the contours down by an amount μ

$$I = \int_{-\infty-i\mu}^{\infty-i\mu} \frac{dp'_4}{2\pi} \int_{-\infty-i\mu}^{\infty-i\mu} \frac{dq'_4}{2\pi} \frac{[2M^2 + \mathbf{p}\mathbf{q} + p'_4 q'_4] e^{-(p'_4 - q'_4)^2 - (\mathbf{p} - \mathbf{q})^2 / \Lambda^2}}{((p'_4 - q'_4)^2 + E_{(p-q)}^2)(q_4'^2 + E_q^2)(p_4'^2 + E_p^2)} \quad (\text{C.2.30})$$

We can now close the contour along the real p_4, q_4 axis, with contour vertices at $(-\infty, -i\mu) \rightarrow (\infty, -i\mu) \rightarrow (\infty, 0) \rightarrow (-\infty, 0) \rightarrow (-\infty, -i\mu)$. The side contours go to zero as $q_4 \rightarrow \pm\infty$. From the residue theorem we know that the integral over the contour is equal to $2\pi i$ times the sum of the enclosed poles. The numerator doesn't effect the poles, so we define

$$F(p_4, q_4) = [2M^2 + \mathbf{p}\mathbf{q} + p'_4 q'_4] e^{-(p'_4 - q'_4)^2 - (\mathbf{p} - \mathbf{q})^2 / \Lambda^2} \quad (\text{C.2.31})$$

The p_4 integral has poles at

$$p_4 = \pm iE_p \quad (\text{C.2.32})$$

$$p_4 = q_4 \pm iE_{p-q} \quad (\text{C.2.33})$$

These poles are only enclosed if $\mu > E_p, E_{p-q}$. To satisfy this, the residues should be multiplied by $\theta(\mu - E_p), \theta(\mu - E_{p-q})$ respectively. Consider the case, $\mu > E_p$. Then the pole at $-iE_p$ is enclosed. So we have

$$I = \int_{-\infty}^{\infty} \frac{dp'_4}{2\pi} \int_{-\infty-i\mu}^{\infty-i\mu} \frac{dq'_4}{2\pi} \frac{F(p_4, q_4)}{((p'_4 - q'_4)^2 + E_{(p-q)}^2)(q_4'^2 + E_q^2)(p_4'^2 + E_p^2)} \quad (\text{C.2.34})$$

$$+ \frac{2\pi i}{2\pi} \int_{-\infty-i\mu}^{\infty-i\mu} \frac{dq'_4}{2\pi} \frac{F(-iE_p, q_4)\theta(\mu - E_p)}{[-2iE_p][q_4^2 + E_q^2][(-iE_p - q'_4)^2 + E_{(p-q)}^2]} \quad (\text{C.2.35})$$

We can now do the integral over q_4 in the same way. This will split I into 4 pieces. The residue enclosed would be $-iE_q$.

$$I = \int_{-\infty}^{\infty} \frac{dp'_4}{2\pi} \int_{-\infty}^{\infty} \frac{dq'_4}{2\pi} \frac{F(p_4, q_4)}{((p'_4 - q'_4)^2 + E_{(p-q)}^2)(q_4'^2 + E_q^2)(p_4'^2 + E_p^2)} \quad (\text{C.2.36})$$

$$+i \int_{-\infty}^{\infty} \frac{dp'_4}{2\pi} \frac{F(p_4, -iE_q)\theta(\mu - E_q)}{[-2iE_q][p_4^2 + E_p^2][(p_4 - (-iE_q))^2 + E_{(p-q)}^2]} \quad (\text{C.2.37})$$

$$+i \int_{-\infty}^{\infty} \frac{dq'_4}{2\pi} \frac{F(-iE_p, q_4)\theta(\mu - E_p)}{[-2iE_p][q_4^2 + E_q^2][(-iE_p - q'_4)^2 + E_{(p-q)}^2]} \quad (\text{C.2.38})$$

$$+i^2 \frac{F(-iE_p, -iE_q)\theta(\mu - E_p)\theta(\mu - E_q)}{[-2iE_p][-2iE_q][(-iE_p - (-iE_q))^2 + E_{(p-q)}^2]} \quad (\text{C.2.39})$$

The first part gives the vacuum contribution. The next 2 give the Lamb shift contribution. The final piece give the exchange contribution. These are the same as what is given in Furnstal et al. multiplied by our gaussian factor.

$$\begin{aligned} \mathcal{E}_{ex} = & \gamma g_s^2 \int \frac{d^3q}{(2\pi)^3} \frac{d^3k}{(2\pi)^3} \frac{\theta(k_f - k)}{2E^*(k)} \frac{\theta(k_f - q)}{2E^*(q)} \\ & \times \left[\frac{E^*(k)E^*(q) + M^{*2} - \mathbf{k} \cdot \mathbf{q}}{(\mathbf{k} - \mathbf{q})^2 - [E^*(k) - E^*(q)]^2 + m_s^2} \right] e^{[(E^*(k) - E^*(q))^2 - (\mathbf{k} - \mathbf{q})^2 / \Lambda^2]} \quad (\text{C.2.40}) \end{aligned}$$

$$\begin{aligned} + \gamma 2g_v^2 \int \frac{d^3q}{(2\pi)^3} \frac{d^3k}{(2\pi)^3} \frac{\theta(k_f - k)}{2E^*(k)} \frac{\theta(k_f - q)}{2E^*(q)} \\ \times \left[\frac{E^*(k)E^*(q) - 2M^{*2} - \mathbf{k} \cdot \mathbf{q}}{(\mathbf{k} - \mathbf{q})^2 - [E^*(k) - E^*(q)]^2 + m_v^2} \right] e^{[(E^*(k) - E^*(q))^2 - (\mathbf{k} - \mathbf{q})^2 / \Lambda^2]} \quad (\text{C.2.41}) \end{aligned}$$